8-2001

The effects of shaft misalignment on efficiency and bearing load of electric motors

Stephen Jesse

To the Graduate Council:

I am submitting herewith a thesis written by Stephen Jesse entitled "The effects of shaft misalignment on efficiency and bearing load of electric motors." I have examined the final electronic copy of this thesis for form and content and recommend that it be accepted in partial fulfillment of the requirements for the degree of Master of Science, with a major in Mechanical Engineering.

J. W. Hines, Major Professor

We have read this thesis and recommend its acceptance:
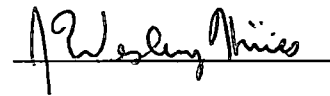
Accepted for the Council:

Carolyn R. Hodges

Vice Provost and Dean of the Graduate School

(Original signatures are on file with official student records.)

To the Graduate Council:
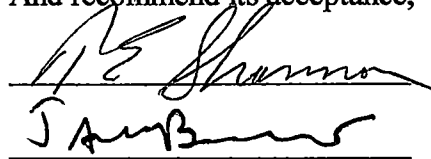
I am submitting herewith a dissertation written by Stephen Jesse entitled "The Effects of Shaft Misalignment on Efficiency and Bearing Load of Electric Motors." I have examined the final copy of this dissertation for form and content and recommend that it be accepted in partial fulfillment of the requirements for the degree of Masters of Science in Mechanical Engineering.

Dr. J.W. Hines, Major Professor

We have read this dissertation

And recommend its acceptance,

Accepted for the Council:

Vice Provost and

Dean of Graduate Studies

The Effects of Shaft Misalignment on

Efficiency and Bearing Load

of Electric Motors

A Thesis

Presented for the

Master of Science Degree

The University of Tennessee, Knoxville

Stephen Jesse

August 2001

Dedication

This thesis is dedicated to my parents

Mr. Reinhardt Jesse

and

Mrs. Ursula Jesse

who have supported me throughout my education

Acknowledgements

Abstract

This thesis examines the characteristics of misalignment of rotating machinery. The first phase of this research determined the effects of motor shaft misalignment on power consumption, and the second phase determined the relationships between motor shaft alignment, roller bearing load, and predicted life. U.S. industry invests significant resources performing precision alignment of rotating machinery. The basis for this expenditure is two assumptions: misalignment causes a decrease in motor efficiency, and misaligned machinery is more prone to failure due to increased loads on bearings, seals, and couplings.

To determine the effects of rotating machinery misalignment on power consumption, controlled experiments were performed at The University of Tennessee and at the Oak Ridge Center for Electrical Machinery System Testing. The testing was performed using a 50 HP and a 60 HP AC induction motor with four different types of flexible couplings. Approximately 15 different alignment conditions were examined for each coupling.

To determine the effects of misalignment on bearing load, sensors were designed, fabricated, and installed into a working motor. These sensors could measure transverse bearing loads in both the vertical and horizontal directions at both the inboard and outboard bearings. The testing was performed using a 60 HP induction motor and four different types of flexible couplings. Testing was performed while the motor was static and while the motor was in operation at full speed and maximum torque.

The results of alignment versus efficiency tests show no significant correlation between misalignment and efficiency when the couplings were operated within the manufacturer's recommended range. Power consumption and power output remained constant regardless of the alignment condition.

The results of bearing load tests show that relatively small amounts of shaft misalignments can have a significant impact on the operational life of a bearing. The magnitude of the bearing life reduction varies with the coupling type, bearing load capacity, and dimensions of the motor. The results from this research show that, in some cases, up to 50% percent of the expected bearing life can be lost with as small as a 5 mil offset misalignment.

Table of Contents

List of Figures

xi

List of Tables

1. Introduction

This thesis will present the results of research exploring the effects of shaft misalignment in electric motors on their reliability and overall operating efficiency. The motivation for this work originally came from a need in industry for scientifically established evidence validating the proposed idea that investing in costly precision alignment will reap greater benefits in the form of energy savings. Previously published work by proponents of this idea had claimed energy savings ranging between 1% to as high as 17% when comparing machinery operating in poorly aligned and well aligned conditions [Daintith 1996, Ludeca 1994, Weiss 1991, Xu 1993], but the evidence supporting these claims was suspect. A collaborative effort between three University of Tennessee Maintenance and Reliability Center (MRC) industrial partners and the University of Tennessee mechanical and nuclear engineering departments sought to answer this question of efficiency by running controlled experiments with the same equipment (motors and flexible couplings) as one might typically find in an industrial setting and performing these experiments in a controlled environment. Previously published work had not explored this question to this extent by putting such a premium on the control and monitoring of all major factors influencing power loss. The end result of this effort showed there to be no measurable power loss as a consequence of shaft misalignment.

Although this finding was not at first readily accepted, it has since been published (and republished) in the three major domestic maintenance oriented trade publications

[Hines, 1997, 1999, 2000] and has also been corroborated by similar research performed at U.S. Naval Laboratories [Gaberson 1998] . In addition, most companies selling alignment equipment have, since the publication of this work, ceased claiming that energy savings is a benefit of precision shaft alignment.

There is however still a key cost benefit to precision alignment, and this is born of improved reliability through reduced loads on roller bearing in rotating equipment. Quantifying this relationship was the focus of the second major objective in this research. In order to do this, sensors were developed and installed in an electric motor which could measure forces induced on the bearings by the shaft while the motor was operating at full speed and under full load. The impact of even a relatively small misalignment was shown to have a large impact on roller bearing life expectancy.

1.1 Overview of Maintenance

In today's competitive industrial climate, the desire to reduce operating costs and improve product quality has brought with it a need to focus on developing more efficient and effective maintenance methods. The responsibility for insuring that effective maintenance procedures are used should not only belong to those people performing the maintenance; but rather, maintenance procedures require a great deal of complex planning and knowledge in its implementation and should be the responsibility of all members in the corporation.

2

Maintenance costs are often considered to be the largest controllable cost for a company, and these expenses can range from between 4% and 14% of operation costs depending on the type of plant [Pardue 1996]. Therefore, it is of paramount importance that resources spent on maintenance are used efficiently and effectively. Striving to achieve this goal has brought with it an evolution in maintenance procedures which center around four maintenance philosophies:

Reactive maintenance involves fixing machinery only after it has failed. Preventive maintenance philosophies schedule activities based on predetermined intervals. Predictive maintenance philosophies monitor machinery condition to determine when maintenance procedures are necessary. Proactive maintenance philosophies attempt to determine and eliminate the root causes for machine failure. In a quest to improve plant reliability, availability, and to reduce maintenance costs, companies are moving away from reactive maintenance regimes towards proactive regimes.

1.1.1 Reactive Maintenance

From the first time that machinery was used in production until the early 1970's, nearly all maintenance procedures, aside from periodic lubrication, was intent on fixing or replacing machinery only after it had exhausted its useful life. Except for the fact that no initial investment in maintenance equipment or personnel training is required for its application, there appear to be few advantages in a reactive approach to maintenance. Such a methodology is inefficient because a plant must have a

constant supply of resources waiting and ready for any kind of failure to occur. Such a method is also expensive. If machines are allowed to undergo catastrophic failure, they can often destroy other machines in their vicinity. Also, a broken machine can halt an entire production process, and lost production results in lost revenue. Lastly, such a method is unsafe. It is literally "an accident waiting to happen". In the same way that a poorly maintained component can destroy nearby machinery, it can also pose a significant health risk and cause irreparable damages. It is impractical and unwise for any company to secure so much of its assets in machinery, production capacity, and personnel in a maintenance approach such as this one.

1.1.2 Preventive Maintenance

Advancements in computer technology in the late 1970's allowed for the capability to archive the type and time of maintenance requirements in a given plant and create a maintenance schedule based on this data. Such a system would estimate the life expectancy of a component based upon the life span of previous components of a similar type. And this knowledge could be used to anticipate machinery breakdown. This type of maintenance is shown to be far better than reactive type maintenance by reducing unanticipated breakdowns [Emmery 1996]. On average, maintenance costs dropped by about 30%, and this method soon became (and still is) the most widely accepted and widely practiced in industry [Pardue 1996].

Whereas a reactive type approach could be thought of as inadequate, a preventive approach to maintenance can be considered excessive. A preventive approach also

4

assumes that there is a repeatable correlation between the age of a component and the likelihood for a failure of that component. This can result in repairs being made to machinery that have not failed or have little threat of failing. With a properly performed preventive maintenance technique employed, maintenance has been made more effective, but because unnecessary work is being performed and healthy machinery is being discarded, such an approach also has inherent inefficiencies.

1.1.3 Predictive Maintenance

To solve the problem of over-maintaining equipment, it is necessary to monitor equipment condition based on its current operational characteristics (not on its age). This predictive or condition based maintenance philosophy is based on the proposition that machinery will give warning signs before failure. These signs may be excessive vibration and noise, increased temperature, or possibly a change in composition or consistency of machine lubricants. If equipment throughout a plant is monitored for such signs, and the condition of equipment throughout a plant is known, then maintenance requests can be planned efficiently and effectively.

1.1.4 Proactive Maintenance

To further improve upon the practice of maintenance it becomes important to not only know if and when a machine will fail, but also to know why a machine would fail. This is a more advanced approach and requires precise, accurate, and comprehensive measurement equipment and expert knowledge to discern what mechanical problems are indicated by the data. This proactive approach attempts to single out the root

causes for a failure and, in a sense, add life to machinery. Two examples of root causes for failure might be imbalance in the rotating machinery or a shaft misalignment between two connected rotating machines. These root causes can be removed resulting in extended machinery life.

1.2 Motivation

The motivation for this work originally came from a need in maintenance organizations for quantitative evidence on which to establish or refine guidelines for the alignment of rotating machinery. Historically, experience and anecdotal evidence primarily guided maintenance procedures. The work presented in this thesis is the result of efforts to clearly define relationships between shaft alignment and energy efficiency and reliability to the benefit of maintenance organizations. With more accurate information, better decision making is possible so that maintenance tasks can be performed in a more cost effective manner.

1.3 Research Objectives

The first objective of this research was to perform tests in an environment where disturbances can be tightly controlled to clarify what relationship truly exists between motor shaft alignment and motor efficiency. In such a setting, the variables effecting motor performance can be either controlled or at least measured. To do this, input power and output power were measured continuously, and steady state operating conditions were maintained during testing. Testing was performed in two different

test facilities with different motors and different measurement equipment, and four different types of flexible couplings were used.

The second objective of this research was to determine, in a quantitative manner, the relationship between motor shaft misalignment and mechanical loads on bearings, and to use this information to predict the impact of these loads on the life expectancy of the bearings. Although this relationship is known to exist and is the primary motivation for precision alignment of rotating equipment, the relationship has never been quantified.

2.0 Shaft Alignment

Shaft misalignment occurs when the centerlines of rotation of two (or more) machinery shafts are not in line with each other, or, more precisely, it is the deviation of relative shaft position from a collinear axis of rotation measured at the points of power transmission when equipment is running at normal operating conditions [Piotrowski, 143]. Shaft misalignment can be divided into two components: offset misalignment, and angular misalignment. As can be seen in Figure 1, and as these names suggest, offset misalignment occurs when the centerlines of two shafts are parallel but do not meet at the power transfer point, and angular misalignment occurs when centerline of two shafts intersect at the power transfer point but are not collinear.
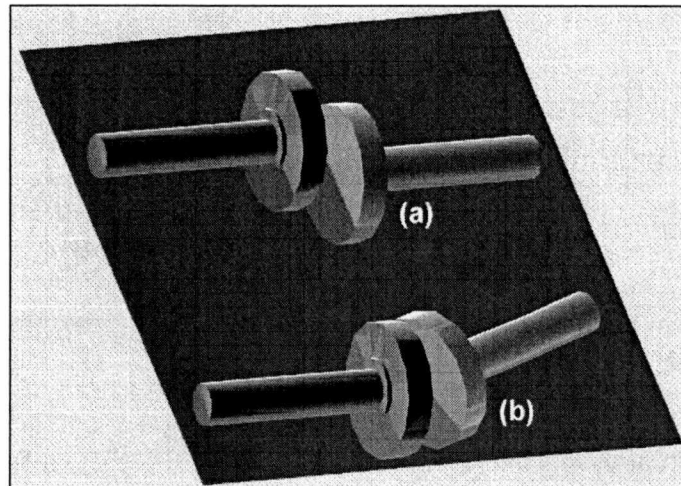
Figure 1: Examples of misalignment (a) offset misalignment and (b) angular misalignment

Often misalignment in actual machinery exhibits a combination of both types of misalignment. We can classify alignment into several grades. Several sources exist for setting these grades including alignment equipment manufacturers, coupling manufacturers, rotating equipment manufacturers, and alignment expert consultants. These grades differ and there seems to be little solid evidence for the setting of these tolerances. We will speak in terms of four grades:

1. Unsafe: Alignments that are outside the coupling manufacturer's operating limits. These tolerances may be between 15-90 mils offset (depending on the type of coupling) for a piece of machinery running at 1800 RPM.

2. Poor: Alignments that are inside the coupling manufacturer's operating limits for the particular coupling but outside the recommended limits for acceptable alignment.

3. Acceptable: Very restrictive alignment tolerance (see following tables).

4. Excellent: Even more restrictive than acceptable rating (see following tables).

Table 1, Table 2, and Figure 2 are three guides for shaft alignment tolerances. One can see that the tolerances given in these guides correlate very well and are quite restrictive. A better standardizing system might be based on the application and equipment involved and on the operating characteristics of the alignment condition.

9

Table 1: CSI recommended tolerances for shaft alignment

RPM	Offset (mils)		Gap (mils/ 10 in)	
	Excellent	Acceptable	Excellent	Acceptable
< 500	5.0	6.0	15.0	20.0
500-1250	4.0	5.0	10.0	15.0
1250-2000	3.0	4.0	5.0	10.0
2000-3500	2.0	3.0	3.0	5.0
3500-7000	1.0	2.0	2.50	3.0
> 7000	0.5	1.0	1.0	2.50

Table 2 : Ludeca recommended tolerances for shaft alignment

RPM	Offset (mils)		Gap (mils/ 10 in)	
	Excellent	Fair	Excellent	Fair
600	5.0	9.0	10.0	15.00
900	3.0	6.0	7.0	10.0
1200	2.5	4.0	5.0	8.0
1800	2.0	3.0	3.0	5.0
3600	1.0	1.5	2.0	3.0
7200	0.5	1.0	1.0	2.0
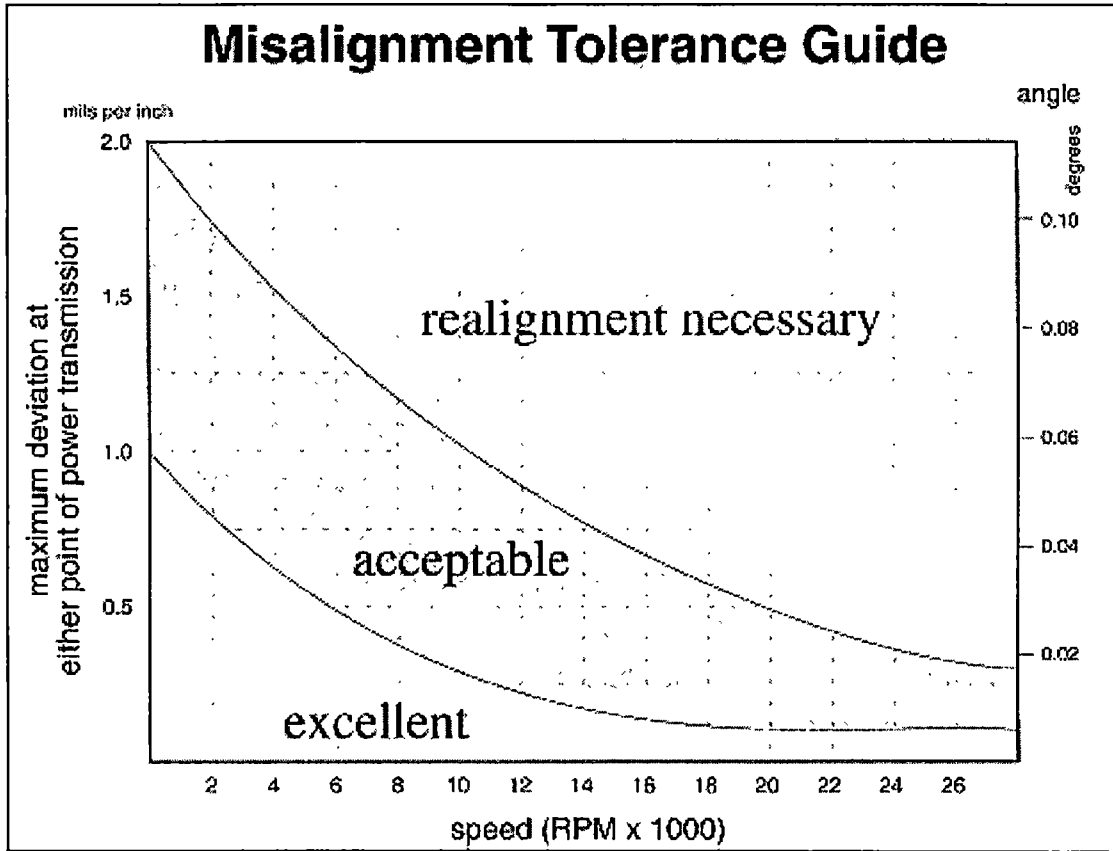
Figure 2: Misalignment tolerance guide from Shaft Alignment Handbook

These characteristics include energy efficiency changes, vibration and temperature changes, and the load and wear on the machinery.

Alignment tolerances are important because this gives technicians a goal towards which to work [Nower]. Without an alignment goal, the technician would not know when the realignment process is sufficiently complete and maintenance managers would not know the alignment condition of the equipment and how these conditions can impact normal operation. Alignment goals need to be realistic and should be based on proven knowledge and experience. If alignment parameters are properly set, a maintenance organization is necessarily more cost and time efficient, and the organization would be properly informed on the positive influence of their work. As can be seen from the previous tables, there is between about a 50% to 100% difference between "fair" and "excellent" standards. This can translate into large differences in the amount of time needed to perform alignment on actual machinery. These are demanding standards to follow and are more stringent than the alignment tolerances set by the manufacturers of flexible couplings.

Measuring misalignments to these tolerances is possible with available technology, but realizing these standards, especially for cases of excellent alignment, in real machinery is difficult and time consuming. This chart specifies what fair and excellent alignment entail, but it is still unknown (to any reasonable degree) what the difference in resulting performance of "excellently" and "fairly" aligned machinery

would be. Is the performance of excellently aligned machinery so much better so as to warrant spending valuable resources on achieving this precision?

2.1 Costs Associated with Precision Alignment

Achieving precision alignment can be, in many situations, a costly and difficult procedure. Achieving proper alignment may require a significant initial investment in expensive alignment equipment and training. Current costs for such equipment range between $500 and $2000 for a dial indicator system and between $10,000 and $20,000 for laser alignment equipment. In addition to this, extensive training of personnel is required to properly operate the alignment equipment. After the initial expense, there are expenses realized when aligning large numbers of rotating machinery in industrial situations. Trained personnel must now be paid to perform alignment and the tradeoffs between labor costs and alignment tolerances become a significant economic issue. For large plants, improving motor shaft alignment can be a continuous process. Changes in a plant environment such as thermal growth of machinery, uneven settling of the building foundation, wear in bearings and couplings and replacement of bearings, couplings, and other components are constantly reintroducing misalignments which need to be continuously corrected. Even with the advent of advanced laser alignment equipment, performing alignment may be a difficult task. Generally the machinery is heavy and its movement may be limited by physical obstructions such as bolt binding. Problems with "soft foot" can arise if the feet of the base of the motor are not plane which would cause alignment to change when bolts are tightened. If there is corrosion or dirt between the motor feet

and the base to which it is attached, alignments could easily shift unexpectedly during the alignment procedure, or even after the bolts have been tightened. All of this can introduce added stresses in the motor casing and increase the uncertainty in alignment measurements, and these problems must be remedied before alignment can be performed correctly.

Shaft alignment can deviate in several ways. There can be offset misalignment in the vertical and horizontal directions, angular misalignments in these directions, and any varied combination of these misalignment cases to be diagnosed and corrected. The degree to which these misalignments are to be corrected has a large impact on the amount of time needed to perform alignment. Performing alignment is an iterative process requiring several steps of making measurements and adjusting the position of machinery. An initial move may result in an alignment close to the desired tolerance and the move itself may be completed in a matter of minutes. Many more iterations might be needed to achieve perfect alignment, or something very close, and may require hours of work. This increased time may take resources away from other maintenance demands in a plant and increase downtime of machinery. Inevitably, the decision must be made as to how well a given piece of rotating machinery needs to be aligned to be considered "good enough". The questions are raised as to how good is "good enough", and how necessary is "perfection".

2.2 Improved Motor Efficiency as a Proposed Benefit

One rationale generally given for performing precision alignment is that system power efficiency will increase with improved alignment. This notion is founded in the belief that couplings and bearings operating in a misaligned state and under increased loads (induced by the increased misalignment) will consume more power than those operating aligned. This power consumption is presumably the result of increased vibration in machinery, or is possibly due to frictional or hysteretic losses in flexible couplings. Previous research relating efficiency increase to alignment has been performed, and the results of this research is summarized below.

2.2.1 Previous Research on Efficiency vs. Alignment

Previously published literature comparing shaft alignment and motor power consumption all agree that efficiency will increase with improvements in alignment. Sources claim 1%-17% electrical power savings resulting from improved alignment, but the variations in ranges of increased efficiency are as numerous as the methods used in determining these values. Many of the sources conducted experiments on mechanical systems operating on-line, in a plant environment where supply and output power and many other critical determinants in motor performance were subject to change. Other reports of decreased power consumption result from more controlled test situations. But even in these tests, input power was often determined by amperage alone and output power was not measured at all, but rather assumed to be constant.

2.2.2 Published Experimental Results

In one experiment, motors and pumps in an operating HVAC system were aligned. After alignment, current required by the motors dropped by between 1 and 18 amps depending on machine[Daintith 96]. Such results are remarkable, but the methods by which they were determined were less than scientific. This experiment was by no means performed in a controlled environment. An HVAC system is, by design, subject to change based on changes in its surroundings. Therefore, power requirements of the system were not constant, and subsequently, input power to the system was not constant, and changes in power consumption can not be attributed to misalignment alone. Also, the only parameter measured to estimate power consumption was current. This is an incomplete description of power consumption if no measurement of voltage is made. This is analogous to trying to measure the speed of a car by recording only the distance traveled and paying no attention to the time required to cover this distance. This lack of information is treated by assuming that voltage is constant. If this were true, there is still another aspect of power supply which must be considered. This is that voltage imbalance between the three phases has an appreciable effect on motor efficiency [Kueck, 1996]. If this is neither controlled nor measured, the validity of the experiment is lost. One possible reason for the large drop in current draw may be found by looking at the procedure of these tests. It is likely that current measurements for the misaligned case were made after the motor had been running for a long time. If the motor was then turned off so that alignment measurements could be made, the rotor and stator windings would have

had a chance to cool. If current consumption measurements were made directly after the motor had been realigned and turned on again, the motor would be running with cooler rotor and stator windings resulting in lower electrical resistance in the windings and a higher motor efficiency. In such a case, the efficiency increase is due to lower operating temperatures of the electric motor, not alignment conditions.

Another published experiment performed in a more controlled environment found power input savings of between 1.3% and 8.7% [Ludeca 94]. In this research, power input to a 3 hp motor was recorded for the misaligned and aligned cases for the motor with no load and then with a 25% load. In this experiment, as in the previous, no measurement of output power was made. So, recorded changes in input power could very likely be due to fluctuations in load on the motor instead of power consumption of couplings and bearings operating in a misaligned state. But, even if output power is assumed constant, closer investigation reveals that the power consumption is very small. For the zero-load case, 8.7% savings were realized. This is out of a total load of about 0.4 hp. This means that about .03 hp more was consumed in the misaligned state. Similarly, the case with the motor at 25% load demonstrated 1.3% savings when aligned. This means that .01 hp more was consumed in the misaligned state [Weiss 91].

2.2.3 Theoretical Estimates of Misaligned State Power Consumption

In addition to experimental results, mathematical models describing angularly misaligned systems have been offered to validate claims of improved efficiency [Xu

17

93]. In this model, the torque in the misaligned input shaft is treated as a vector. This vector is divided into two orthogonal components. As shown in Figure 3, one component is parallel to the output shaft, and the other is perpendicular to it.

In this model, the assumption was made that all torque in the perpendicular component is lost and can in no way transmit power to the output shaft. This is a significant assumption and its validity is questionable. Flexible couplings are designed to transmit oblique torque. To claim that all power is lost may over-simplify the problem and ignore vital information. But, if this assumption is maintained, it is then possible to calculate power loss from the lost torque. The author does this and tabulates data comparing power loss to angular misalignment.
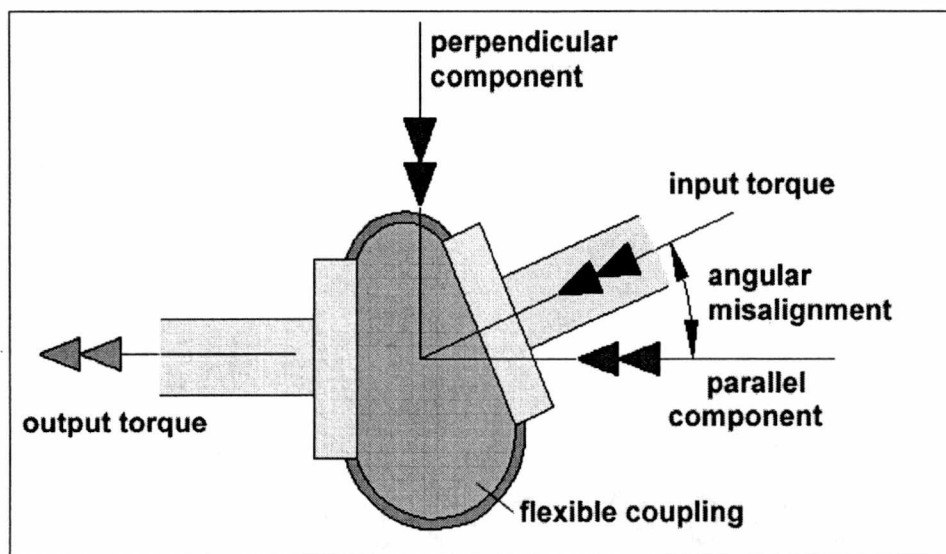
Figure 3: Theoretical misalignment model

One example using the table is given in order to demonstrate loss of power due to misalignment. In this, a hypothetical facility has 25,000 hp of installed rotating machinery operating at a cost of $0.08/kWh. On average, these machines are misaligned 4 mils/inch and can be aligned to .5 mils/inch. If these machines were run continuously for one year, results show a savings of $ 45,750. These appear to be large savings. But when compared with the total cost of a $13 million electric bill to operate the machinery, the results are somewhat less impressive showing a 0.3% savings in electric costs. If this is weighed against the expense of performing alignment for what might possibly be hundreds of motors, the proposition that precision alignment can save money by reducing power consumption seems less likely.

In general, previous research agrees that proper alignment of rotating machinery improves efficiency, but the evidence that is given to support these claims is not conclusive and the extent of power savings is inconsistent. The means by which these results were found can not be considered reliable as many important factors effecting and describing motor performance were neither controlled nor measured in the case of experiments or completely ignored in the case of theoretical estimates.

2.3 Increased Life Expectancy of Machine Components as a Proposed Benefit of Precision Alignment

The other reason for precision alignment relates to the fact that mechanical loads on mechanical components such as bearings, seals, shafts, and couplings decrease with improved alignment. These reduced loads result in less wear on and longer life expectancy of machine components. This can have a large impact on the overall operation of a plant. If the time between failure of equipment can be increased, less regular maintenance would be required for existing machinery. Figure 4 shows the results of a previous study depicting the impact of misalignment on machine life [Piotrowski].
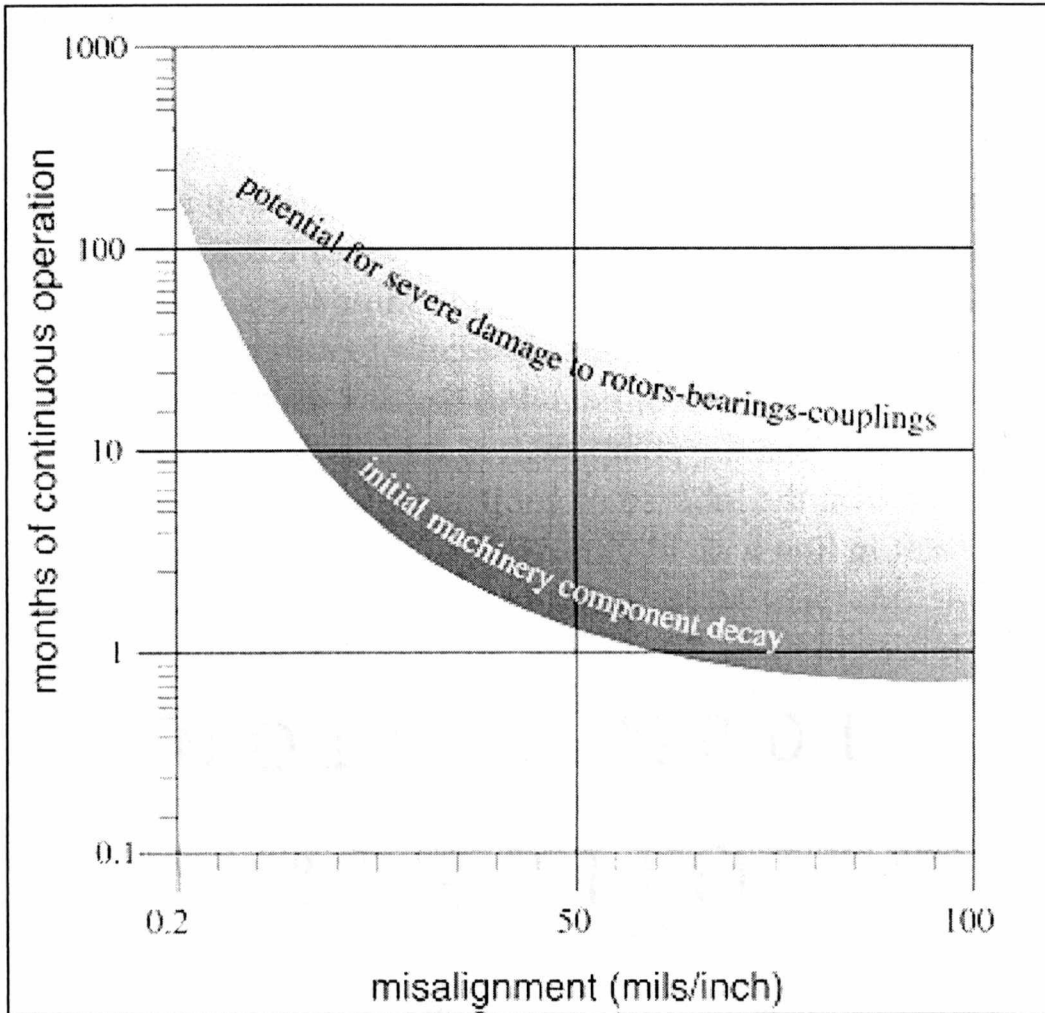
Figure 4: Misalignment vs. machine life from <u>Shaft Alignment Handbook</u>

3.0 Methodology

The experimental setups for the two phases of this project are similar. Differences in setup or configurations specific to a given phase of research are clearly noted.

3.1 Experimental Set-up For Efficiency testing

Many steps were taken in the design of experimental set-ups and procedure to avoid pitfalls encountered by previous experiments regarding efficiency. Testing was performed at two facilities using separate measuring systems so that results from either site could be verified. One round of testing took place at the Oak Ridge Center for Electrical Machinery Systems at Oak Ridge National Laboratories, and the other at the University of Tennessee Mechanical Engineering Engine Laboratory.

3.1.1 The Motor and Dynamometer at UTK

Testing was performed using a 60 hp, 3 phase, 480 volt A/C electric motor. The motor drove a D/C dynamometer rated at 300 hp. Table 3 shows nameplate specifications of the motor and dynamometer.

Table 3 : Motor and dynamometer at UTK facility

GE Model No. 5k326Al115			
60 hp	230/460	3 phase	60 Hz
Service Factor	1.15	3555 rpm	
40 amps max			
Bearing:	roller....		
1 7/8 in shaft dia.	(keyed)		

GE type TLC-3544	
Generator:	300 hp
motor:	250 hp
316 V	635 amps
2500/5000 rpm	
Bearing	Journal

Figure 5 shows the motor and dynamometer setup at the UTK facility. In this set-up, the electric motor was bolted to an 18" X 18" X 1.5" steel plate, the midplate. The four corners of the bottom side of the midplate had 1/4" thick ground and polished steel pads attached to them. The motor/midplate assembly rested on a large 42" X 26" X 4" steel plate.

The top surface of this base plate was also ground to a polished finish. Horizontal alignment conditions were changed by moving the midplate to which the motor was attached over the surface of the base plate. The smooth and flat contact surfaces between the midplate and the base plate facilitated this movement and eliminated the likelihood of soft foot. The base plate was supported by four jack stands at the corners of the base plate. These were used not only for support but also served to adjust the vertical position of the motor with respect to the dynamometer. Figure 6 shows the motor support assembly from above. Four motor position adjustment bolts of 1/4-20 threads were used to move the motor across the surface of the base plate, and the two dial indicators were used to measure this motion in 1 mil increments.

Two thermocouples were positioned inside the stator windings of the motor, with one near the outboard end and one closer to the inboard end. Readings from the thermocouple were used to determine when thermal steady state operation of the system had been reached indicating when testing could begin. Temperature readings were also taken using and infrared pyrometer. This was used to monitor how surface
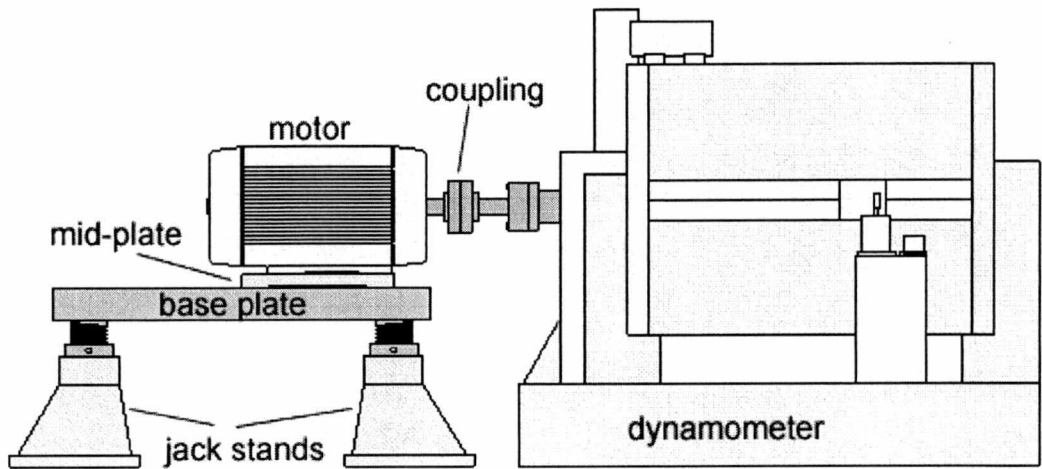
Figure 5: Profile of motor and dynamometer setup
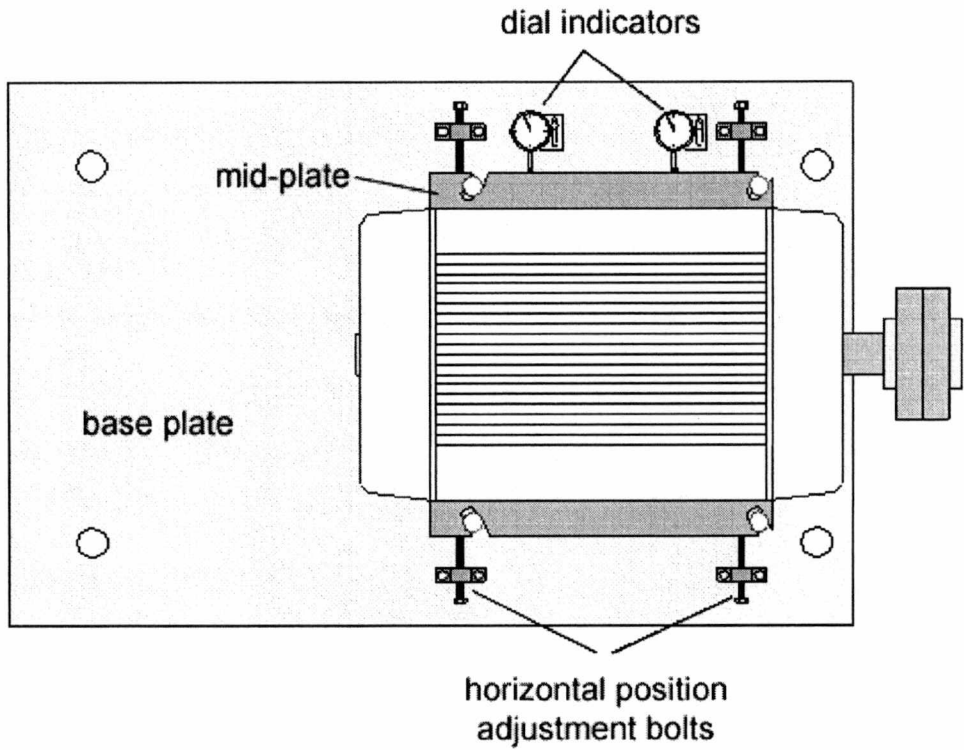
Figure 6: Plan view of motor support.

temperatures at or near the coupling and at the inboard bearing of the motor varied with changes in alignment. Figure 7 shows the locations where temperature measurements were taken.

In addition to efficiency and motor position, vibration, temperature, and motor magnetic flux measurements were taken. Vibration data was taken at ten location. Two accelerometers were placed at the outboard side of both the motor and the dynamometer to measure vertical and horizontal vibration at the bearings. Three accelerometers were placed at the inboard side of the motor and dynamometer to measure vibration in the vertical, horizontal, and axial directions at the bearing.

During the first phase of research, data from vibration, magnetic flux, current, and motor speed were all recorded with a four channel DAT recorder. The four channel
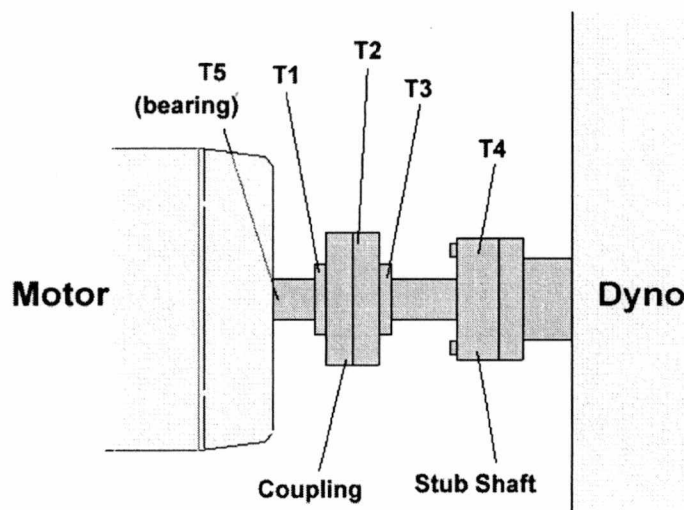
Figure 7 : Location of surface temperature measurements

25

limit presented a problem when 13 sets of continuous data were to be recorded. For this reason, a switch box was used to toggle between the different sets of data. The data was divided in the following manner: two channels of motor outboard vibration and flux coil readings were recorded together, three channels of inboard vibration data comprised the second set, three channels of inboard dynamometer vibration data comprised the third set, and two channels of outboard dynamometer vibration data plus one phase of motor input current data constituted the fourth set of data. Each set of data was recorded for at least 2 minutes before moving on to the next set of data. Figure 8 shows how the data was divided during acquisition.

Uncertainty in experimental measurement of efficiency was estimated by examining the resolution of measurement equipment for input power, output torque, and output
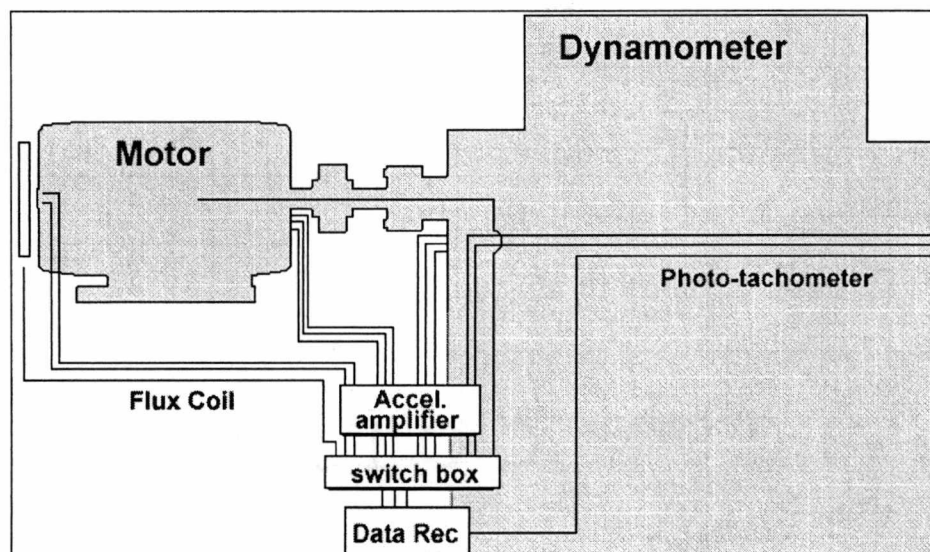
Figure 8: Vibration data acquisition setup at UTK

speed. The calculations for this are shown in the appendix and the results are shown in Table 4.

3.1.2 The Oak Ridge Test Facility

At the Oak Ridge test facility testing was performed using a 50 hp 3 phase 480 volt A/C electric motor. The motor was loaded using a water cooled 150 hp dynamometer. Specifications of the motor and dynamometer are shown in Table 5.

Figure 9 shows the dynamometer setup at the Oak Ridge facility. This design has a lower profile than that used at the University of Tennessee and is more rigid. The motor was attached to a 20" X 20" X 8" block of aluminum. Two threaded rods fitting into the aluminum block were used to adjust motor position in the horizontal plane. Figure 10 shows the aluminum motor support clamped in place by four levers. The levers were supported on one end and held down through their center bolts. Off line measurements were made using CSI's UltraSpec laser alignment system. Thermal growth measurements were made using permanently installed CSI lasers and verified using Eisenger bars.

As in the UTK setup, vibration was measured at ten locations on the motor and dynamometer. Two accelerometers near the motor and dynamometer outboard bearings measured vertical and horizontal vibration, and three accelerometers on the motor and dynamometer inboard bearings measured vertical, horizontal, and axial Data from the vibration accelerometers, magnetic flux coil, three phases of electrical

Table 4: Uncertainty in motor efficiency measurements at UTK

	approx.value		uncertainty			
Input Power	50	kW	0.05	kW	0.10	%
Output Speed	3600	rpm	0.5	rpm	0.01	%
Output Torque	90	ft-lbs	0.1	ft-lbs	0.11	%
Efficiency	0.9	-	0.0014	-	0.15	%

Table 5: Motor and dynamometer at the Oak Ridge facility

Reliance Electric			
I.D. No.	22MN324503 G 001 SY		
Model No.	P3264503A	Volts	230/460
HP	50	Amps	118/59.3
RPM	3550	Phase	3
Bearing:	55BC03J 30X	Design B	Type P

Dynamatic	
Model No.	AD-8080
Serial	40001-213-6
Capacity	150 hp
Speed	2600-9000 rpm
Bearing	roller
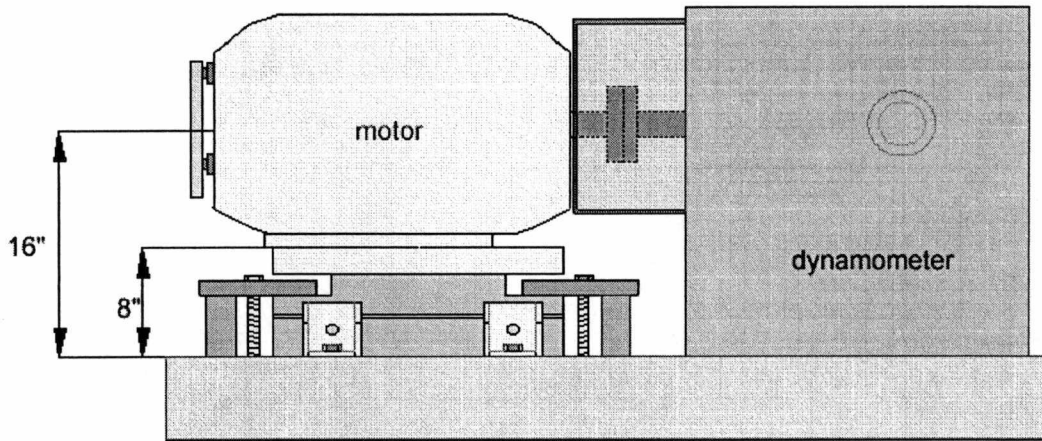
Figure 9: Motor and dynamometer setup at Oak Ridge
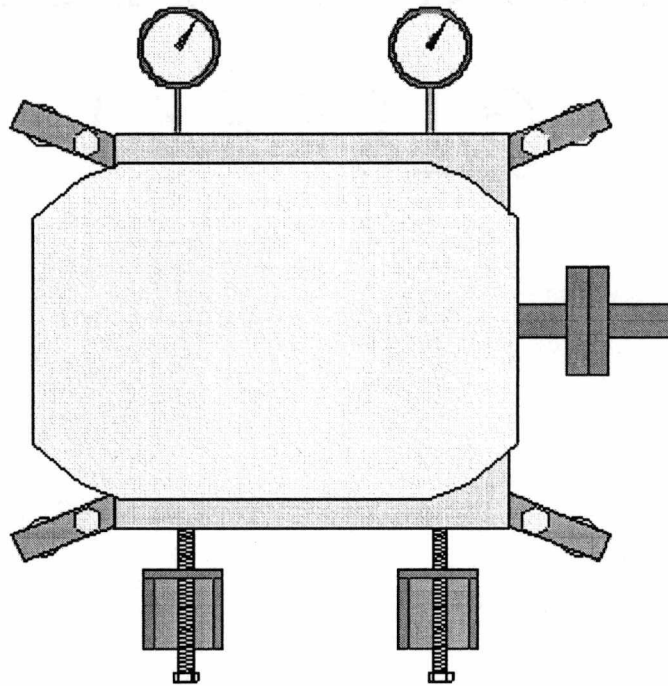
Figure 10: Plan view of motor support

vibration. Motor magnetic flux was measured at the motor outboard endbell.

current data, three phases of voltage data, were recorded on an 8 channel TEAC

digital tape recorder. The overall accuracy of the motor efficiency measurements at

ORNL's motor test lab was determined by taking the square root of the sum of

squared accuracies of individual measurements such as speed, torque, current,

voltage, and phase angle. The overall accuracy was ± 0.5 %.

3.2 Flexible Couplings Used During Testing

There were four types of flexible couplings used during testing. These couplings were

suggested by Duke Power Company as being the most commonly used types within

their industry. They are shown below in Table 6 with the manufacturer's

specifications for maximum angular and offset misalignments.

Figure 11 through Figure 14 show the approximate appearance of these couplings. In

each of these figures part (a) shows a cross-sectional view and dimensions of the

actual couplings used during testing, and part (b) shows isometric views of couplings

of a similar type but not exactly like those used in testing.

Table 6: Manufacturer's tolerances for flexible couplings

Type	Manufacturer	Model	Max. Offset	Max. Ang.
Grid	Dodge	1060T	12	120
Elastomer (tire)	Rexnord	ES10R el, 10SHRB hub	70	400
Link Pack	Zurn	3011/2GP	26	80
Gear	Zurn		50	150
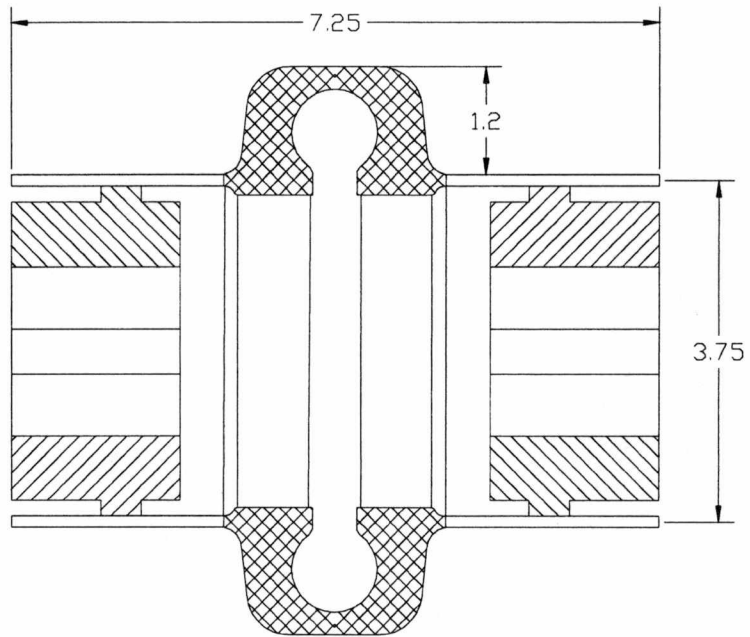
(a)
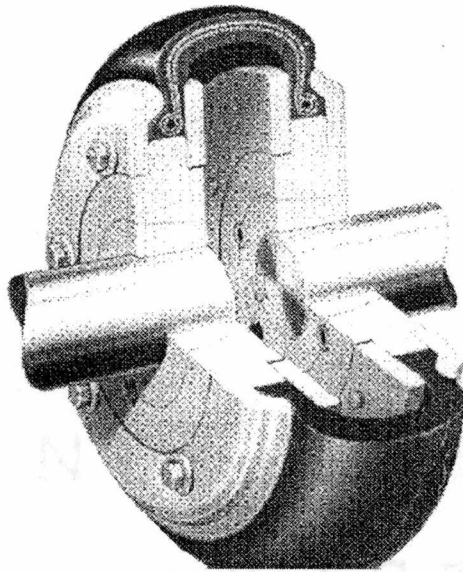
(b)

Figure 11: Tire or elastomeric type coupling
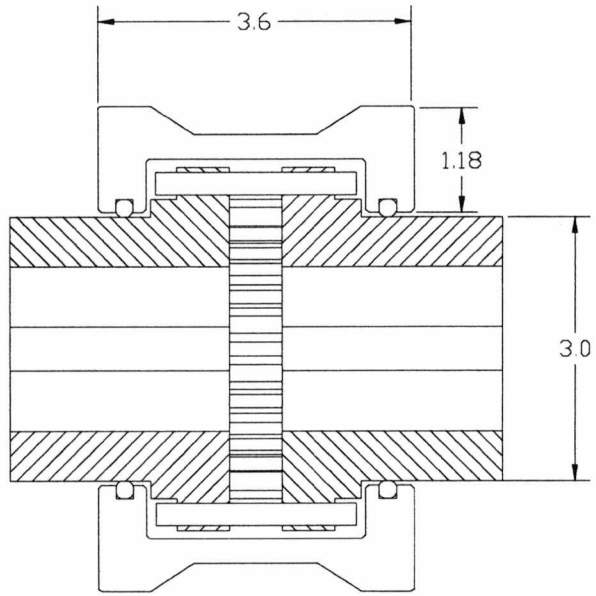
(a)
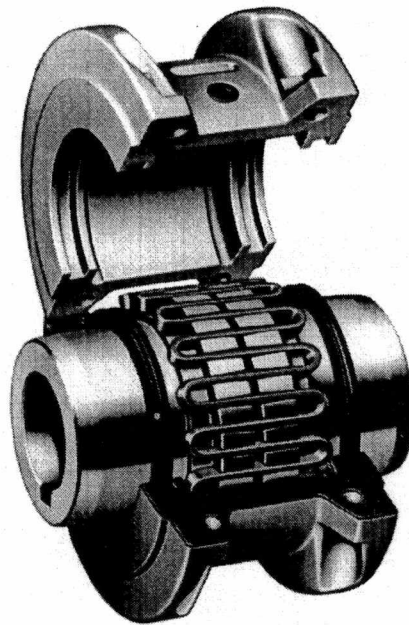
(b)

Figure 12: Grid or ribbon type coupling
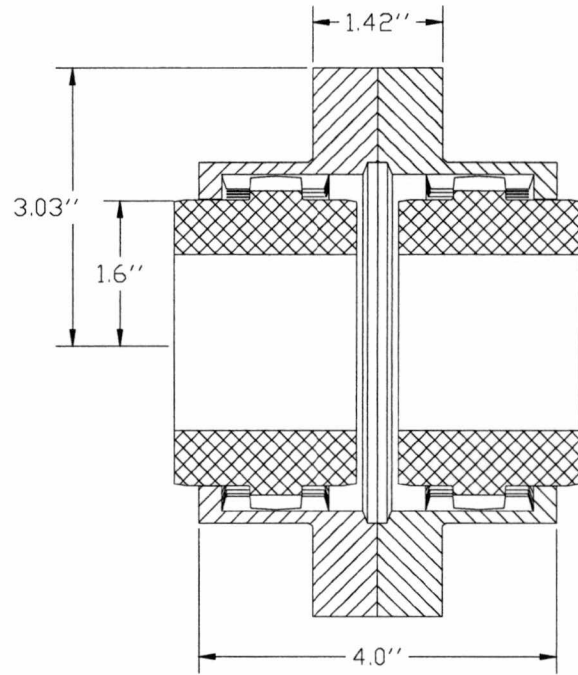
(a)
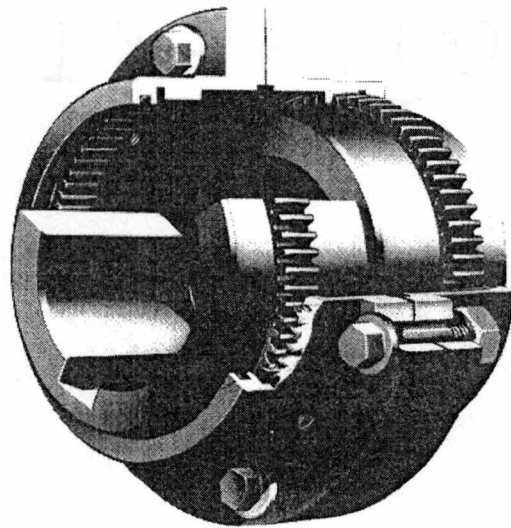
(b)

Figure 13: Gear type coupling
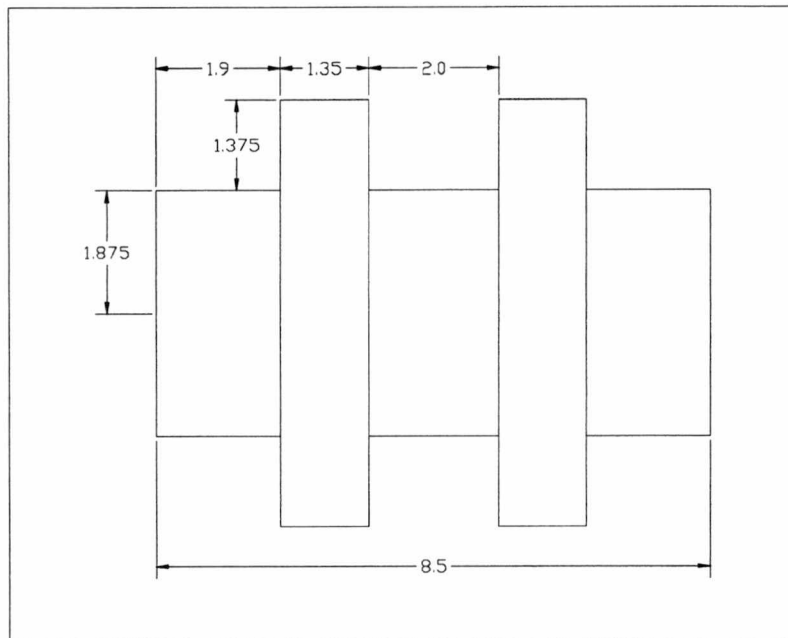
(a)
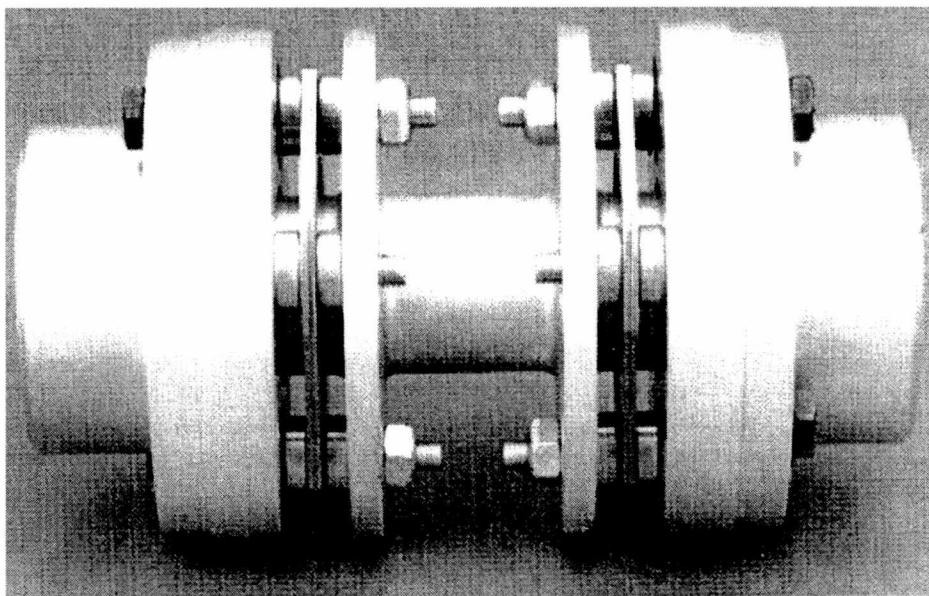
(b)

Figure 14: Flexible link coupling

3.3 Bearing Load Sensors

3.3.1 The Design of Sensor Rings

The research objectives and approach of the second phase of research appear to be unprecedented. A literature survey has found no previously published work which attempted to relate shaft misalignment through flexible couplings to bearing load by measuring forces directly at the bearings. Therefore, a new type of load measuring device was conceived and developed to meet the needs of this project.

Some of the requirements necessary for proper operation of the load sensors are as follows: the sensors

- needed to operate under full load and at full speed motor conditions,

- were required to be strong and reliable so as not to yield during the operation of the motor even while operating under extreme misalignment conditions,

- needed to be sensitive enough to detect appreciable variations in load, should not interfere with the operation or structural integrity of the motor

- in any noticeable way,

- needed to be as temperature independent as possible so that the large variations in motor temperature did not interfere with bearing load data collection,

- should be designed in such a manner as to allow for both the magnitude and direction of the forces on the bearing to be determined.

Several load measuring device designs were considered ranging from measuring strain in the rotating shaft, to refitting the motor with load sensing end bells, to finding actual bearings with load sensing capabilities built into them, to trying to measure loads at the motor feet and extrapolating these measurements to forces at the bearings. None of these options appeared to satisfactorily fulfill the initial design requirements.

A final design concept was chosen in which a sensing interface (sensor ring) was placed in the motor between the shaft bearings and the supporting structure of the rotor. However, this configuration requires that some space be "created" between the outside of the bearing and the inside of its housing. This space can be provided either by removing material from the end bells in which the bearings are housed or by replacing the original motor bearing with one having a smaller outer diameter. The latter approach was chosen.

Figure 15 shows the components and the assembly process for the outboard bearing sensor. In this figure, part A is the original bearing. Part C is the replacement bearing having the same inner diameter of the original bearing, but a smaller outer diameter. In the case of the outboard end of the motor, the original ball bearing was replaced with a needle roller bearing. Part B is the sensor ring, to which the strain gages were attached. The outer diameter of B matches that of the original ball bearing, and the inner diameter of B is the same dimension as the outer diameter of part C. Parts B
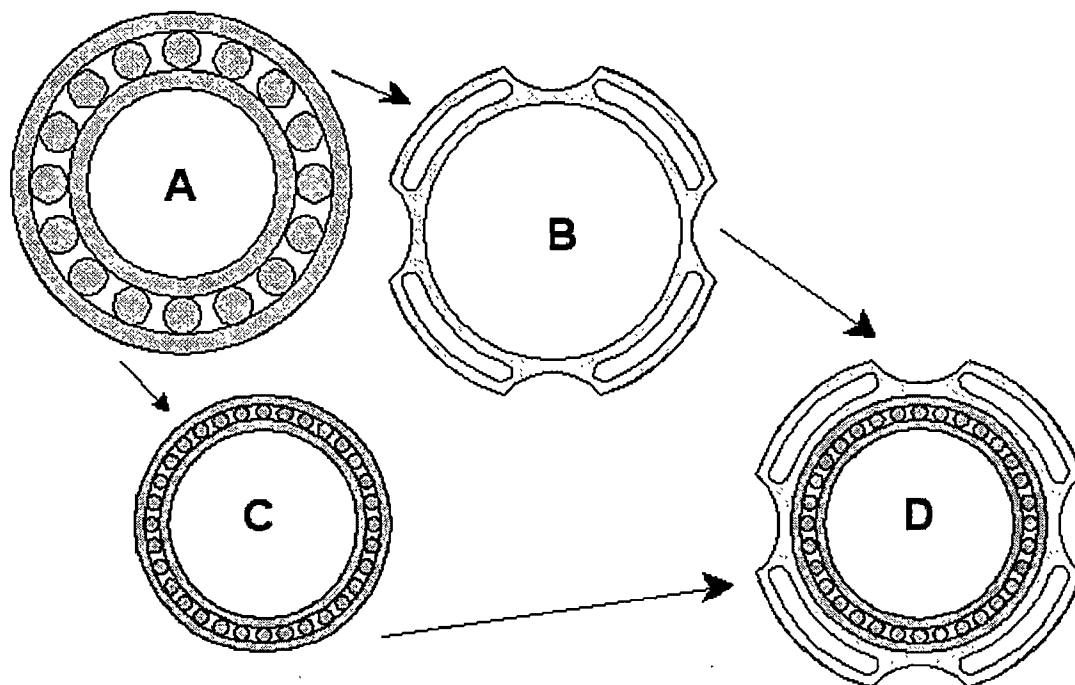
Figure 15: Replacement of original bearing and assembly of sensor ring

and C are press fit together to form part D, and D then replaces the original bearing in the assembly of the motor.

Design of the actual rings was an involved process itself. Balancing strength against sensitivity, stress localization against overall deformation, and functionality against size constraints required multiple iterations. Construction and testing of these various design concepts would have been entirely impractical, and the complex geometries of the proposed designs were too complicated for standard mechanics of materials theory to handle with necessary accuracy. The alternative and indispensable tool in this design process was finite element analysis (FEA). The software COSMOS/M was

used to perform the FEA computations, and the results of these calculations helped in determining adequate sensor ring configurations and insuring proper functioning of the final design. Figure 16a and Figure 16b show the sensor rings for the inboard and outboard bearings.

The finite element analysis for the chosen sensor designs showed that (at the locations of the strain gages) the inboard bearing would strain approximately 0.29 μin/in when a 1 lbf. load was applied to the interior side of the bearing sensor closest to the strain gage. The outboard sensor would strain approximately 0.21 μin/in under the same conditions. The estimated yield strength of the sensors is about 1500 lbf. of transverse bearing load.

There was a design oversight in the original plans of the sensor rings. Initially, it was expected that the pressed fit between the sensor rings and the original bearing housing would be sufficient in eliminating any slippage between the sensor and bearing housing. Upon initial testing of the sensor rings, it became obvious that further measures had to be taken to secure the sensors to the bell housing. Slippage at specific locations (Figure 17) was interfering with strain/load measurements and creating an artificial and falsely perceived load measurement hysteresis.
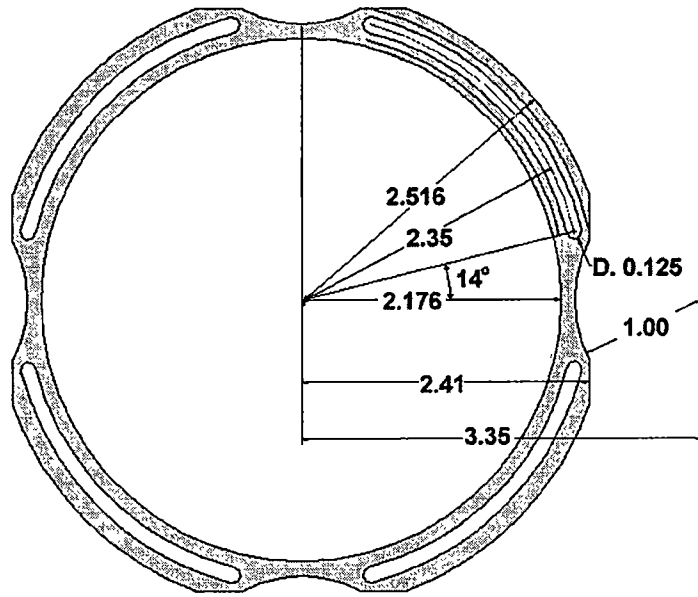
(a)
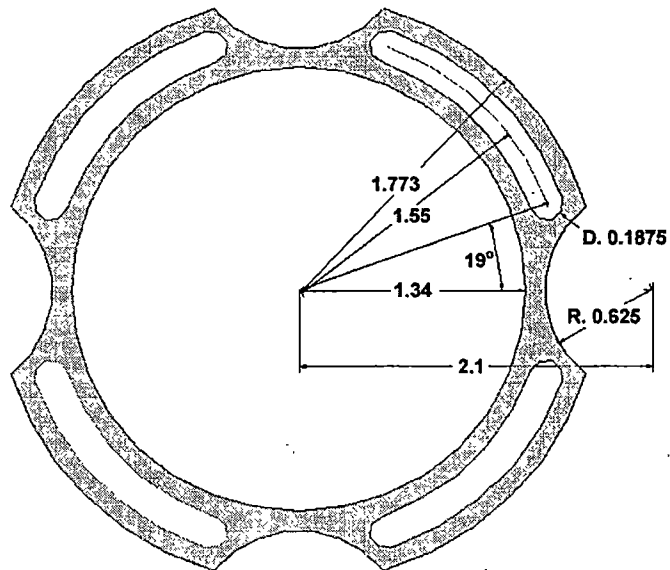
(b)

Figure 16: Construction of sensor rings, a) outboard , b) inboard
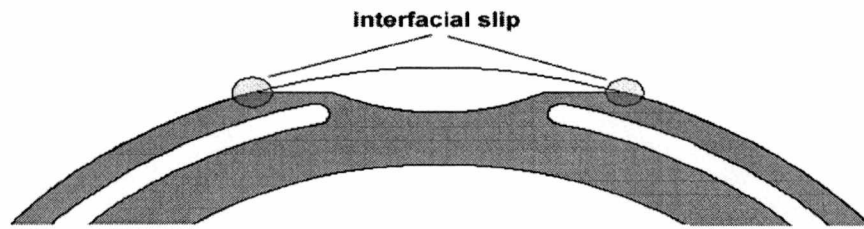
Figure 17: Likely location of inter-surface slippage

This problem was remedied by drilling and tapping several holes into the sensor rings and through the original bearing housing (Figure 18). (These 8,1/8 in diameter holes were the only permanent changes made to any part of the motor). The sensor rings could then be bolted to the bearing housing thus eliminating any noticeable slippage.

3.3.2 Discussion of Strain Gages

Force induced strain in the sensor rings was converted to voltage signals by way of strain gages located at several locations around the sensor rings. The strain gages were assembled in temperature compensating, full bridge configurations. Five thermocouples were placed in close proximity to the bearings to measure temperature changes there. These thermocouples were used to confirm that the load measurements were temperature independent. There was a total of four full bridges per sensor ring. The strain gages were positioned as close to the centers of stress concentrations as possible in order to maximize measurement sensitivity. These locations are depicted below in Figure 19a and b. R(red) and B(black) signify the excitation voltage leads and W(white) and G(green) are the signal leads. Specifications of the strain gages are shown in Table 7.
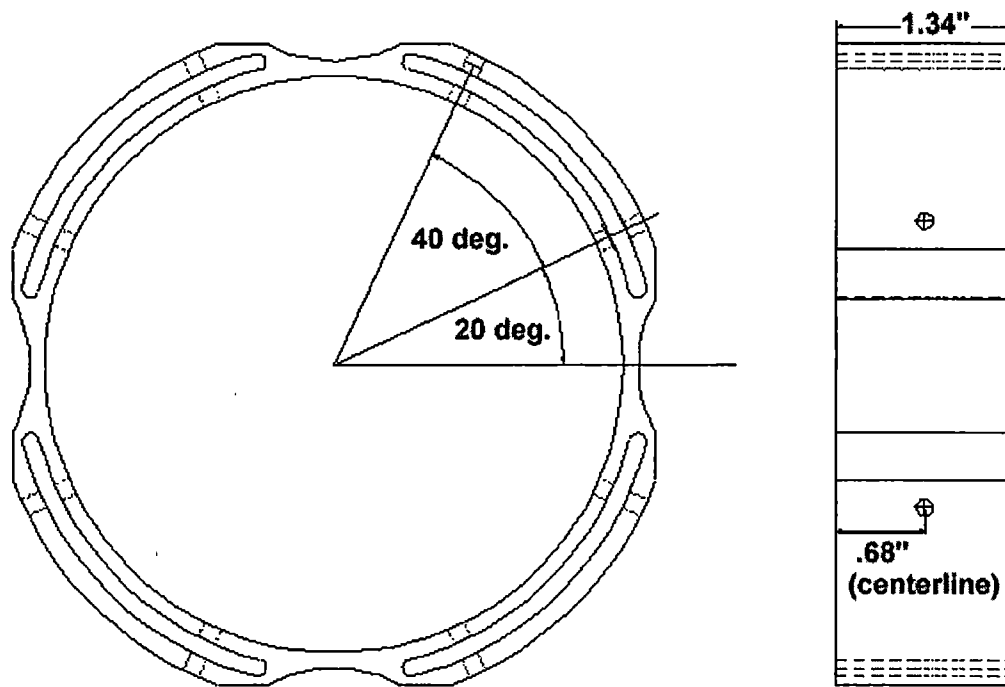
Figure 18: Location of stabilizing bolts in sensor rings

(a)

(b)
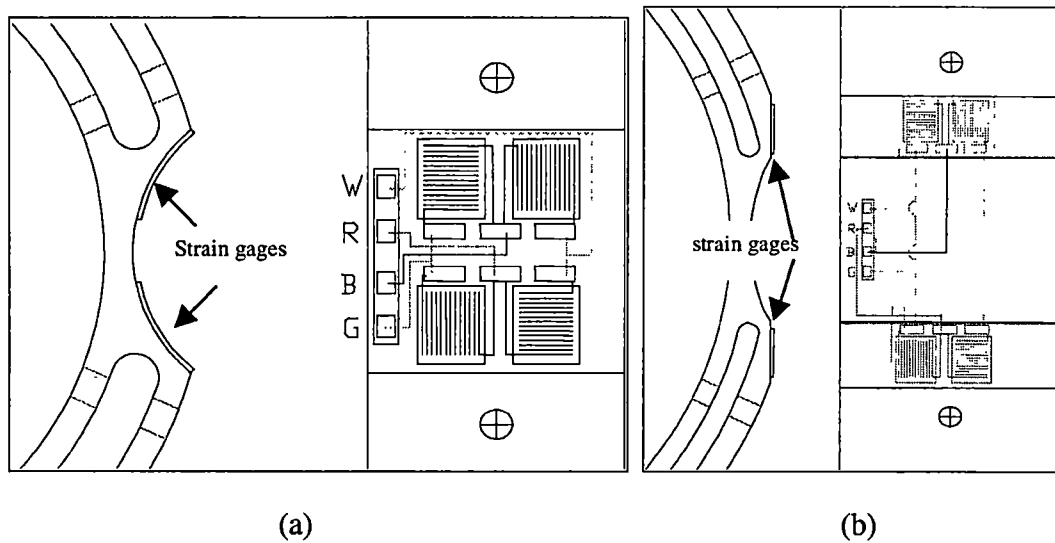
Figure 19: Strain gage location and configuration, (a) outboard, (b) inboard

41

Table 7: Specifications of strain gages

Manufacturer:	Measurement Group, Inc.
Type:	EA-06-125TB-350
Resistance:	350.0 ± 0.2 % Ohms
Gage Factor:	2.07 ± 0.5 %

The excitation voltage during all measurements was maintained at 9.51 Volts. Figure 20 shows the full bridge strain gage arrangement in schematic form and as the actual arrangement used in the load sensors.

Equation 1 relates changes in strain gage bridge output voltage and can be calculated based on strain in the material, material characteristics, and gage characteristics. Equation 2 uses the known characteristics used in this project to calculate the anticipated sensitivity of the bearing sensors to a given load.
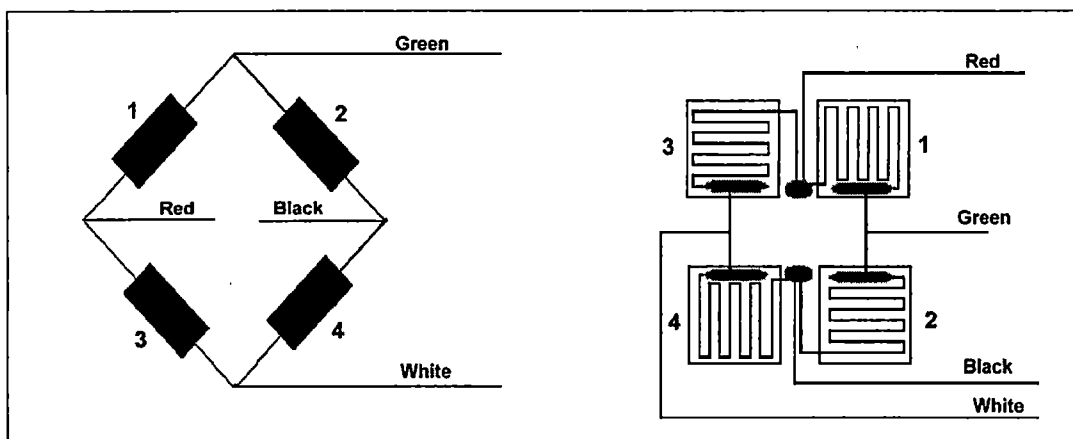
Figure 20: Strain gage arrangement for full bridge

$$E_o = E_i \cdot \left(\frac{R_1}{R_1 + R_2} - \frac{R_3}{R_3 + R_4} \right)$$

$$\delta E_o = E_i \cdot \frac{GF}{4} \cdot \left(\varepsilon_1 - \varepsilon_2 + \varepsilon_4 - \varepsilon_3 \right)$$

R_n = Resitance in gage n

E_o = measured voltage

δE_o = change in E_o

$\varepsilon_{metal} = \varepsilon_1 = \varepsilon_4 = \varepsilon$

$\varepsilon_2 = \varepsilon_3 = -\varepsilon_1 \cdot \nu = -\varepsilon \cdot \nu$

E_i = excitation voltage

GF = gage factor

ε_n = strain in gage n

ν = poisson's ratio

$$\delta E_o = E_i \cdot \frac{GF}{4} \cdot (\varepsilon - (-\nu \cdot \varepsilon) + \varepsilon - (-\nu \cdot \varepsilon))$$

$$\delta E_o = E_i \cdot \frac{GF}{2} \cdot \varepsilon (1 + \nu)$$

Equation 1: Strain gage equations

$$E_i = 9.51 \cdot V \qquad GF = 2.07 \qquad \nu = .3 \qquad \varepsilon = 0.29 \cdot 10^{-6} \cdot \left(\frac{in}{in} \cdot \frac{1}{lbf} \right)$$

$$\delta E_o = \frac{1}{2} \cdot E_i \cdot GF \cdot \varepsilon (1 + \nu)$$

$$\delta E_o = 3.71 \cdot 10^{-6} \cdot \frac{V}{lbf}$$

Equation 2: Applied strain gage equations

43

3.3.3 Data Acquisition

All load data was acquired via an amplifying data acquisition (DAQ) board, Table 8.
Because of the weakness of the incoming voltage signal, a high level selectable gain
capability was critical to the operation of the data acquisition system. For all strain
measurements, the DAQ board was configured for 8-differential channels (required
for multiple strain gage measurement) and monopolar voltage range at 1000X
amplification. These settings, coupled with the 12 bit resolution, allowed for voltage
sensitivity of 2.44×10^{-7} volts/bit. With such sensitivity no other external
amplification was required or used. This insured that no outside data filtering or
signal attenuation could interfere with data acquisition. Data filtering is often desired
in analog to digital data acquisition, but it should be noted that, for this project, there
was no need to analyze signal frequency by fast Fourier transform or by any other
means. Therefore, no anti-aliasing filtration was necessary to protect signal integrity.
All undesirable noise was filtered by means of successive averaging in post-
processing.

Table 8: Specifications of data acquisition board

Manufacturer:	CyberResearch, CYDAS 1601
Resolution:	12 bit
No. Channels:	16-single ended, 8-differential
Maximum Sampling Rate:	160 kHz
Voltage range:	10 V, bipolar/monopolar
Selectable Gains:	1,10,100,1000X

44

In-line, strain gage bridge balancing circuitry was necessary in order to keep signal voltages between the restrictive 0 to .01 V range dictated by the setting on the DAQ board. The circuit diagram in Figure 21 shows the simple method by which this was accomplished by bridging the ground excitation lead to one of the sensor leads via a 1 M-ohm variable resistor. This circuit was repeated for all of the strain gage bridges in the set-up.

The data acquisition board could record a maximum of 8 differential signals. There were eight possible load signals that could be recorded, but for parts of the experimentation (dynamic testing), it was necessary to also record the angular position of the rotor shaft by way of a photo-tachometer signal. To accommodate this, one of the outboard load sensors recording vertically directed forces was omitted, and the photo-tachometer signal was recorded in its place.
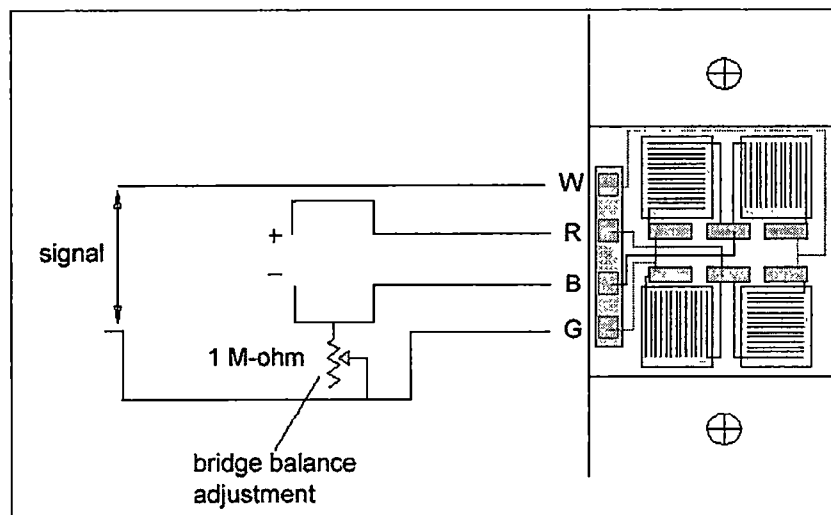
Figure 21: Bridge balancing circuit

All programming and interfacing between the computer and the data acquisition

board was accomplished within the Hewlett-Packard HP-VEE visual engineering

environment software package.

3.3.4 Calibration of Sensors

Figure 22 illustrates the calibration set-up used to correlate sensor signals to

magnitudes and directions of forces on the shaft (the bearing loads). The set-up

consists of a large metal ring positioned concentrically with the shaft of the motor and

held securely to the same base as the motor. Sixteen evenly spaced holes around the

circumference of the ring provide one end of a connection point for load inducing

springs. The other end of this spring is connected to the motor shaft via a turn-

buckle. The magnitude of the radial force on the shaft can be varied by adjusting the

overall length of the turn-buckle/spring, and the direction of the force simply depends

on angular positioning of the outer end of the spring.
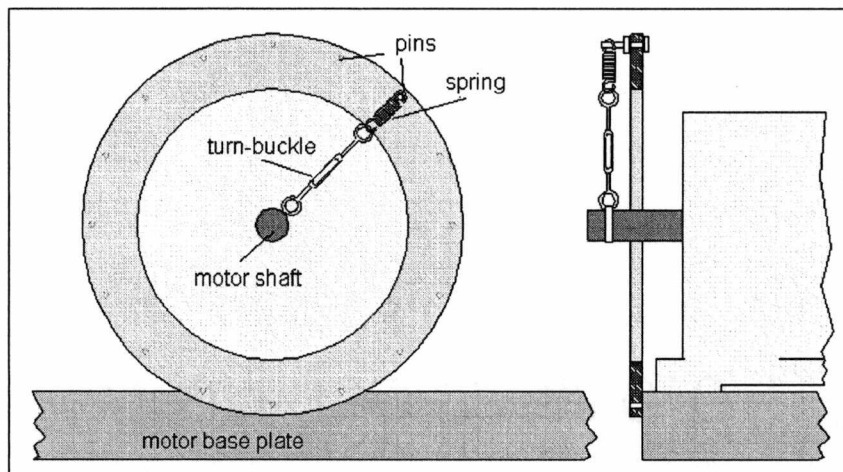
Figure 22: Sensor calibration set-up

The calibration procedure consisted of measuring sensor signals over a range of loads from 0 to about 300 lbs., in 22.5° increments over the full 360° around the motor shaft for both the inboard and outboard shafts of the motor. A small extension to the outboard end of the shaft was fabricated and installed for outboard sensor measurements. Also, a separate, simpler set-up was devised to similarly induce axial loading in the rotor shaft. This testing showed the sensor rings to be entirely insensitive to axial load. As much as 500 lbs. of axial load was placed on the shaft with no measurable response detected in the load signal.

3.3.5 Results of Calibration Testing

The results from the calibration procedure showed that the sensors would satisfactorily fulfill their design requirements. As stated previously, it was important that the sensors maintain linearity over a large range of force magnitudes. Figure 23 shows a plot relating inboard vertical sensor signal to a vertical load. The "R^2" value describing deviation from the best fit trend line is close to unity indicating a high degree of linearity over the range of measured loads. Also, the slope of the trend line shows that the sensitivity to load is adequate at 0.66 bits/lbf., or inversely, about 1.5 lbf./bit. This means that the experimental set up can detect changes in load in increments of 1.5 lbs. This level of sensitivity and linearity was the same in the horizontal measurements as well. Outboard sensors offered resolution of about 2.5 lbf./bit.

Vertical Sensor Readings vs. Vertical Load

$y = 0.6622x$
$R^2 = 0.999$
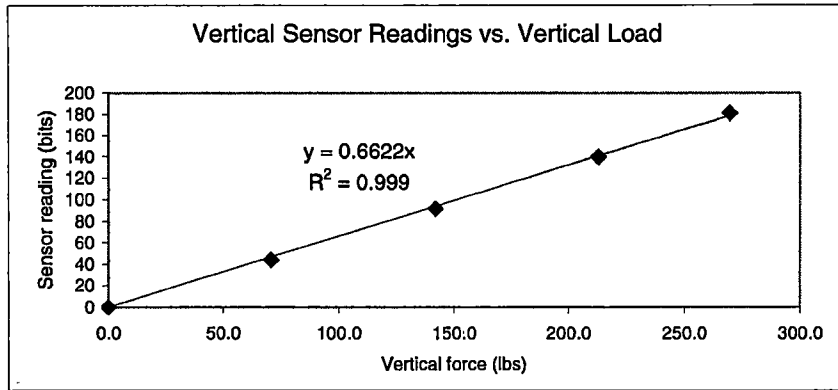
Figure 23: Plot showing linearity and sensitivity of force transduction

Another important, but not critical, aspect of this specific sensor arrangement

concerns what can be described as "orthogonality". During the initial phase of design

of the sensor rings, there was concern that the overall unusual geometry (skewed

strain gage angles, odd stress distributions, etc.) might cause sensors intended for

measuring load in only one direction (for instance vertical) to detect loads in a

perpendicular direction (in this case, horizontal, or even axial). If such

interconnectedness were evident in the sensor ring, interpretation of the signals would

be far more difficult. Calibration tests have shown instead that sensors intended to

measure load in one direction are only 1.0% as sensitive to load perpendicular to that

direction. The orthogonality of the geometry and orientation of the sensors is

preserved in their functionality. This means that if the vertical and horizontal load

measurements are known, the bearing load can be determined by simple vector

algebra. Figure 24 shows how the vertical sensor signal of the inboard bearing varies

as the direction of
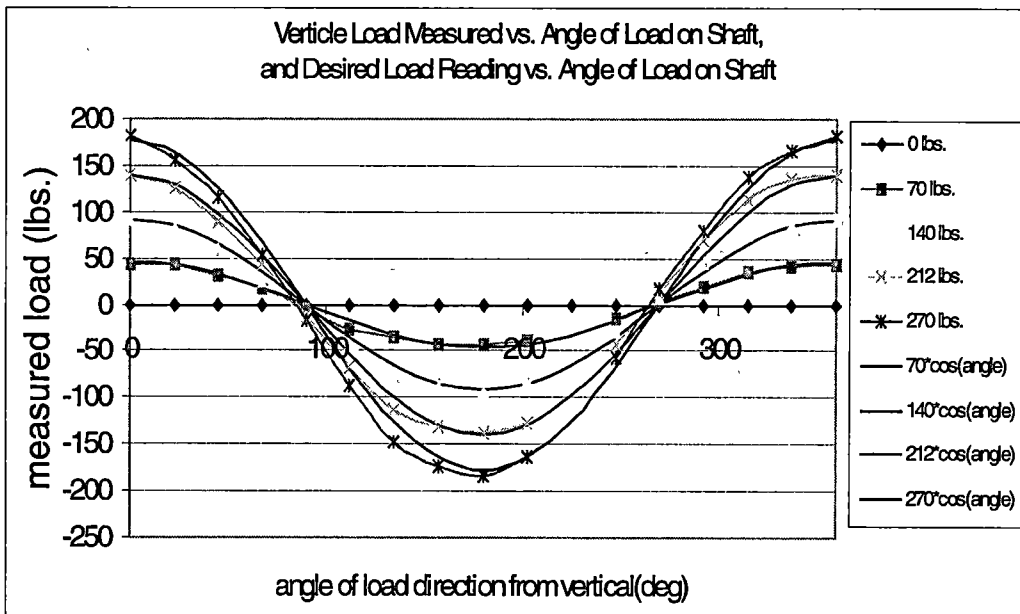
Figure 24: Plot demonstrating orthogonality of sensor signals

the load varies. As expected, this load variation is sinusoidal and closely follows the trend: "vertical force component = (magnitude of force)*(cos(angle with vertical))" .

3.4 Experimental Procedure for Measuring Efficiency

The objective of the experimental procedure in the first phase was to measure changes in motor performance related to changes in shaft alignment. The alignment was varied from a perfect alignment to a maximum misalignment condition to within the manufacturer's specified limit. Figure 25 shows how the manufacturer's information on pure angular and offset misalignments was used to define maximum misalignment conditions for cases when offset and angular misalignments were combined. As can be seen in this graph, a plot is made showing test misalignment conditions where angular misalignment is plotted against offset misalignment. If a line is drawn connecting the maximum allowable pure misalignments, all test conditions were limited to the region within that line and the axes of the graph.
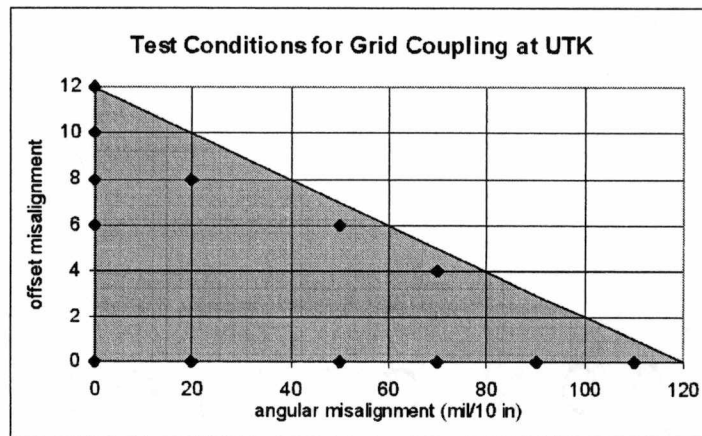
Figure 25: Example showing how angular and offset misalignments were combined

3.4.1 The Experimental Procedure at the University of Tennessee Facility

Experimentation began by first calibrating the dial indicators using the shaft mounted laser alignment equipment. This involved zeroing the dial indicators when the motor was aligned in the horizontal plane. Then, the motor was moved through the range of predetermined alignment conditions and the dial indicator readings were recorded for each of these conditions. The motor was then repositioned and aligned with an allowance made for thermal growth in the vertical direction. After this, the motor was started and the dynamometer was adjusted to apply a full load on the motor. The motor was then allowed to reach steady state operating conditions. The criteria for having reached steady state involved monitoring the temperatures in the stator windings and waiting until the rate of temperature change was less that 1.0 degree Fahrenheit per 30 minutes. This generally required about 2 hours. All tests using the four different couplings were performed in essentially the same way. The only difference between procedures was the variation in the magnitude of misalignments. These magnitudes were determined based on the coupling manufacture's recommended maximum allowable misalignments.

With the motor under full load, and running at a constant speed of 3560 rpm and the temperature of the motor stabilized, testing was begun. The first base-line measurements were made with the motor aligned. Input power, current, voltage, and power factor were measured using a power meter sampling at 10 kHz and averaging these values continuously over 10 second periods. Output torque and shaft speed were

51

then measured. From these values, efficiency could be calculated. Three efficiency calculations in intervals of about 2.5 minutes were made for each alignment condition. During this time, 2 minutes of vibration, magnetic flux, a tachometer pulse signal, and current data was archived to the DAT recorders.

Except for the first tests performed at the UTK facility involving the gear coupling, all changes in motor alignment were made while the motor was operating under full load. This insured that the operating conditions of the motor such as temperature of the motor windings would remain constant throughout the testing period. To perform this fully loaded move, the bolts attaching the midplate to the base plate were loosened slightly, and the motor was pushed to the next alignment condition using the motor position adjustment bolts. The bolts connecting the midplate to the base plate were tightened, and another set of tests could begin. In the case of the gear coupling tests at UTK, the motor was turned off before it was moved. This had the unfortunate effect of allowing the motor to cool down, and therefore an additional hour of warm up time was required between each alignment condition before testing could resume. The end result was that conditions, including line voltages, were less consistent and the efficiency calculations were more variable.

Efficiency measurements for one coupling type over the range of alignment conditions could usually be completed in one day. Testing began by measuring the effects of pure offset misalignment on motor performance, then pure angular

misalignment on motor performance, followed by several tests where offset and angular misalignment conditions were combined. Throughout testing for a given coupling, the motor was often returned to the aligned condition to assure that no instrumentation drift was interfering with data collection.

3.4.2 Experimental Procedure at Oak Ridge Facility

Apart from a few differences resulting from different instrumentation, the experimental procedure was essentially the same for the two test sites. There were no thermocouples placed in the stator windings of the motor at the Oak Ridge facility so criteria for steady state operation based on temperature could not be used. Instead, the motor was run under full load for the entire night (at least 8 hours) preceding testing. This more than insured steady state operation. Measurements for three phases of input voltage, three phases of input current, shaft speed, and output torque were sent directly to a computerized data acquisition system. The data was sampled at a rate of 5 kHz and averaged over 10 seconds to calculate efficiency.

3.5 Experimental Procedure for Measuring Bearing Load

Performing the actual bearing load testing was fast and simple once all of the sensors and data acquisition systems were operating correctly. The experimentation was divided into three categories: static testing, steady state testing, and dynamic testing. The data acquisition set-up was the same for each of these different types of tests. In all cases, data was sampled in blocks at a rate of 6000 Hz per channel for 5 seconds.

The difference between these types of tests lies mainly in the operation of the motor and dynamometer and the post-processing of the data.

3.5.1 Static State Test Data Collection

The objective of static state testing was two fold. The static state testing provided a safe way to insure proper operations of the test equipment (load sensors, data acquisition, test procedure etc.). This testing provided a preview of the types of bearing loads one could expect in misaligned machinery while it was running. Static tests also gave a data set against which the steady state results could be compared.

Static tests were performed while the motor was not running, but with the motor coupled to the dynamometer as if the motor were ready to run at full speed and under full load. The motor was always perfectly aligned (to within ±1 mil offset, and ±1 mil/10 in. angular) before testing began, and a baseline measurement was always taken in this aligned case before load measurements were made with the motor misaligned. A block of data was sampled under various alignment conditions, the average sensor value over the 5 sec sampling span was calculated and recorded. There were often as many as 25 to 50 sets of the averaged sensor signals recorded per alignment condition. When there appeared to be sufficient agreement within the sets of averaged data for a given alignment condition, the motor was moved to the next alignment condition, and load measurements were repeated.

All changes in alignment were made in the horizontal plane. Misalignment conditions were varied in the following order for each of the four types of couplings:

1) up to maximum positive pure offset misalignment

2) combination of positive offset and positive angularity

3) up to maximum positive pure angular misalignment

4) combination of negative offset and positive angularity

5) up to maximum negative pure offset misalignment

For each of these cases, data was taken at 4 or 5 evenly spaced alignment conditions between the aligned and maximum misaligned conditions.

3.5.2 Steady State Test Data Collection

Collecting and analyzing the steady state test data was the main focus of the bearing load analysis . The findings from this portion of the research gave information on how much additional load was imposed on the bearings while the motor was running in a misaligned state. This information could then be used to predict life of the bearing.

The steady state testing was performed almost identically to the static testing with the only difference being that the motor was running under full speed and full load conditions while measurements and alignment changes were made. There was also an approximately 1 to 2 hour warm up period needed before testing could begin in which the motor could reach a constant operating temperature.

3.5.3 Dynamic Test Data Collection

The purpose of dynamic testing was to examine whether the cyclic loading on bearings varied or could be correlated to changes in misalignment. As in steady state testing, dynamic data collection occurred while the motor was running. In fact, steady state and dynamic test data was taken at approximately the same time. However, the dynamic data was not averaged before it was stored. The high frequency oscillatory nature of the bearing load was captured, therefore, exposing the manner in which bearing load varied over one revolution.

4.0 Discussion of Results

4.1 Results of Motor Efficiency Testing

The results of this research show no measurable change in motor efficiency related to motor shaft misalignment when the tested couplings were operated within the manufacturer's recommended range. Power consumption and power output remained steady regardless of motor position. If power consumption did fluctuate, as sometimes was the case at the UTK facility, this occurred independently of alignment conditions. It is possible that changes in motor efficiency do occur as a result of shaft misalignment, but any changes that might be evident were smaller than the resolution of the measurement equipment. It should also be reiterated that the tested couplings were not taken beyond their maximum recommended misalignment operating condition as may sometimes occur in applied in-use situations where alignment is not carefully checked. In these extreme cases, losses may perhaps be higher. But in such cases, the cost incurred by earlier and increased damage to machinery would generally far outweigh the increased power consumption.

4.1.1 Results from Experimentation at UTK for Efficiency

Table 9 shows the compiled results from testing at the University of Tennessee. As can be seen from these results, there is no clear and measurable correlation between alignment conditions and efficiency. For the case of the tests performed at UTK,

57

variations in motor efficiency did occur as a result of poor quality line voltage. The results of the gear coupling test performed at UTK showed the greatest variations in efficiency. But, as mentioned previously, this is most likely a result of intermittent starting and stopping of the motor. It should also be mentioned that this was the first coupling tested and that this testing took place over a span of several weeks. The testing with other couplings was usually completed within the span of several hours.

4.1.2 Results from Experimentation at ORNL for Efficiency

Table 10 shows the results from motor efficiency testing at the Oak Ridge Facility. As seen previously in the UTK results, there is no clear and measurable correlation between motor alignment and efficiency. There were changes in motor efficiency readings that did occur as a result of problems with measurement equipment and are explained.

There was a problem with instrumentation drift in the load cell used to measure output torque during efficiency tests using the grid coupling. It is clear that the changes in measured efficiency were a result of drift in measurement equipment and not related to shaft misalignment because realigning the system as the last alignment condition did not change efficiency.

An error occurred in shaft alignment during testing of the gear coupling at ORNL which required that the motor be turned off. The drastic jump in efficiency recorded

Table 9: Compiled data for alignment vs. efficiency tests at UTK

Rexnord Coupling				Grid Coupling				Gear Coupling				Linkpack Coupling		
Horizontal		Eff.		Horizontal		Eff.		Horizontal		Eff.		Horizontal		Eff.
ang.	offset			ang.	offset			ang.	offset			ang.	offset	
mil/10 in	mils			mil/10 in	mils			mil/10 in	mils			mil/10 in	mils	
0	0	89.4%		0	0	88.8%		1	1	92.4%		0	0	89.7%
0	-15	89.2%		0	6	88.6%		1	-27	92.9%		0	4	89.7%
0	-30	88.5%		0	8	88.3%		1	-46	92.9%		0	8	89.4%
0	-45	88.7%		0	10	87.7%		1	-50	90.5%		0	14	89.5%
0	-45	88.7%		0	12	87.9%		1	1	92.7%		0	20	89.3%
0	-70	88.2%		0	0	88.5%		42	6	90.9%		0	26	89.4%
0	0	88.0%		20	0	88.2%		21	2	90.8%		0	0	89.3%
0	0	89.6%		0	0	89.3%		54	9	91.3%		40	0	88.9%
100	0	89.3%		50	0	89.4%		1	0	91.5%		60	0	89.2%
200	0	88.9%		70	0	89.3%		21	-14	90.7%		80	0	89.2%
400	0	88.8%		90	0	88.3%		20	-37	90.8%		40	12	89.2%
250	-45	89.7%		110	0	88.6%		41	-11	90.8%		40	-12	89.2%
250	45	88.9%		20	8	89.0%		1	0	92.1%		0	0	89.2%
0	0	89.3%		50	6	88.8%		11	-9	90.4%				
				70	4	88.2%		38	-40	90.6%				
				0	0	88.3%		29	1	90.8%				
								3	2	90.0%				
								59	2	90.6%				
								154	0	90.5%				
								100	2	90.5%				
								2	1	90.3%				
								2	1	89.9%				
								42	-20	90.3%				
								62	-29	90.7%				
								84	-38	90.3%				

Table 10: Compiled data for alignment vs. efficiency tests at ORNL

Grid Coupling			Gear Coupling			Rexnord Coupling			Link Coupling		
Horizontal		Eff.	Horizontal		Eff.	Horizontal		Eff.	Horizontal		Eff.
offset	ang.		offset	ang.		offset	ang.		offset	ang.	
mils	mil/in		mils	mil/in		mils	mil/in		mils	mil/in	
0	0	87.7	0	0	89.5	0	0	89.3	0	0	88
0	4	87.7	0	6	89.4	15	0	89.3	4	0	88
0	8	87.7	0	12	88.8	30	0	89.4	8	0	88
0	12	87.7	0	15	88.7	45	0	89.3	14	0	87.9*
4	0	87.9	20	0	88.7	60	0	89.4	20	0	85.4*
4	4	87.9	21	0	87.9*	70	0	89.4	0	0	90.4*
4	8	87.9	0	0	89.4*	0	0	89.2	26	0	90.4
4	-8	88.1	35	0	89.2	0	10	89.2	0	4	90.4
8	0	88.2	50	0	89.2	0	20	89.2	12	4	90.3
8	4	88.2	-20	10	89.1	0	40	89.1	-12	4	90.3
8	8	88.2	*motor shut down			45	25	89.3	6	6	90.3
8	12	88.2	and restarted			-45	25	89.3	0	8	90.3
0	0	88.2							20	2	90.3
*small drift in load cell									*faulty current probe		

60

during this test is a result of the motor being turned off and the load cell being recalibrated.

During efficiency testing of the flexible link coupling, a faulty current probe interfered with efficiency measurements. This was deemed to be the cause because the sum of the three line currents did not equal the known total input current. When this problem was remedied, efficiency did not change.

4.1.3 Theoretical Estimates of Power Loss Due to Shaft Misalignment

Despite no significant measurable changes in efficiency resulting from poor alignment, there were other notable changes in motor performance. Motor vibration and noise generally increased, the temperature of the coupling increased, the temperature of the bearings increased, and wear on at least one of the couplings increased. These are all common traits of misaligned rotating machinery and components, and are all most likely caused by increased loads experienced by the bearings and couplings. What is also important to note about all of these traits is that energy is required to drive them, energy that must come from input power to the system and must therefore affect efficiency.

It may appear contradictory to claim that misaligned rotating machinery consumes no more power than aligned machinery and simultaneously claim an increase in power-consuming symptoms of misalignment such as vibration and bearing temperature. However, this can be explained using simple calculations showing that the power

61

required to drive damped vibration and temperature increases are insignificant and for all practical purposes immeasurable compared to the power transmitted through a coupling and shaft. Figure 26 is a thermodynamic model of the bearing, shaft, and coupling used for this analysis. The model assumes that when the system is operating under steady state conditions the only power losses that can occur due to misalignment are friction in bearings and couplings resulting in increased heating and dissipation of kinetic energy evident in damped vibration.

4.1.4 Estimated Power Loss Associated with Temperature Increase

The first set of calculations sought to determine the amount of power necessary to increase the temperature of the shaft, bearing, and coupling to the levels measured. In order to do this, simplification of geometry and operating conditions were made, but these simplifications were conservatively biased to produce final theoretical results showing higher power consumption as compared to the actual system. First, it was
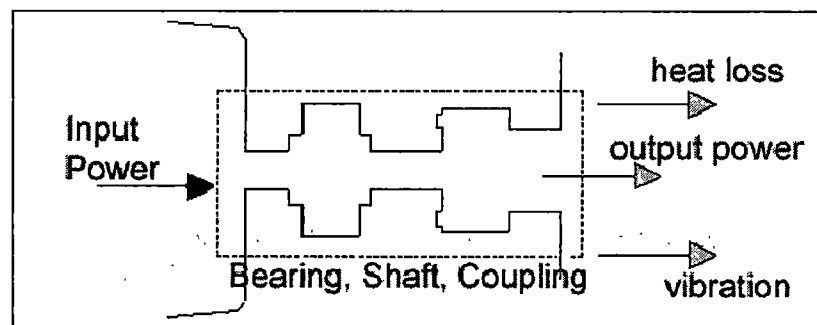
Figure 26: Thermodynamic model of motor shaft

assumed that all heat loss from the shaft was by convection. In order to find convective heat loss based on temperature, it was necessary to determine a coefficient of convective heat transfer between the shaft and the surrounding air. Equation 3 is the relationship between heat and temperature [Incropera, 1990].

$$\Delta q = h_L \cdot A_s \left(T_{misaligned} - T_{aligned} \right)$$

Equation 3

The geometry of the rotating shaft and coupling was represented by a single shaft of constant diameter. The diameter of the hypothetical shaft was larger than the actual shaft, and the length was about 1.5 times that of the original. Increasing these dimensions had the effect of increasing the relative velocity of the air surrounding the shaft and increasing the surface area of contact between the rotating shaft and the surrounding air, thus exaggerating the theoretical heat loss. Figure 27 shows the geometries of the actual shaft and the hypothetical shaft used in the analysis.

In order to use standard equations for convective heat transfer, the rotating shaft was treated as a flat plate. In this analysis, the circumference of the shaft became the length of the flat plate, the length of the shaft became the width of the plate, and the velocity of the surface of the shaft became the velocity of the air flowing over the plate (V_{inf}). For this model, a there was a 3°C temperature increase assumed throughout the entire shaft resulting from misalignment. This greatly overestimates

63
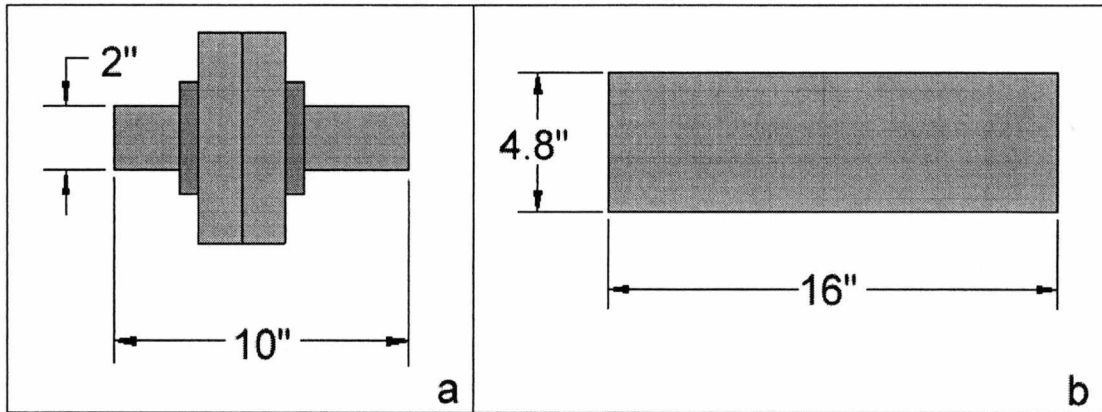
Figure 27: Simplified geometry for the heat loss estimation (a)actual dimensions of shaft and (b) approximated dimensions of shaft

what was recorded during experimentation in two ways. First, there was no increase in temperature resulting from misalignment as large a 3°C at any point on the shaft for any of the alignment conditions. Second, the temperature increase that was recorded was not distributed evenly throughout the shaft. Instead, temperature increases were very localized in close proximity to the bearing.

By using the previously mentioned simplifications and assumptions and standard values of air for viscosity, conductive heat transfer, and Prandlt number, the heat loss due to convective heat transfer was found to be about 32 Watts. This is equal to only .065% of 60 hp transferred through the shaft. Despite all of the assumptions in the model that grossly overestimate the heat transfer capabilities of the actual system, the energy required to drive the temperature increase has been shown to be insignificant.

4.1.5 Estimated Power Loss Associated with Increased Vibration

The second set of calculations were used to determine the amount of energy required to increase the vibration to levels measured during testing. Vibration itself does not consume energy. Energy is consumed when vibration is damped and converted to heat as a result of hysteresis within the vibrating material. This heat would be distributed throughout the motor, not just in coupling which was discussed in the previous section. Equation 4 was used to calculate power loss in a damped oscillating system [Thomson, 1981].

$$W_d = \pi \cdot \zeta \cdot \beta \cdot k \cdot \left(x_{ma}^2 - x_a^2 \right)$$

Equation 4

This equation is valid only for a single degree of freedom system where W_d is the increase in power dissipated per cycle due to damping, ζ is the damping coefficient, β is the ratio between the driving frequency and the natural frequency of the system, k is the spring constant, x_{ma} and x_a are the magnitudes of displacement of the oscillating mass in the misaligned and aligned state respectively. As before, it was necessary to simplify the physical problem in order to calculate the required power. The most significant simplification involved reducing the three dimensional problem to single degree of freedom system so that Equation 4 could be used. This was done by ignoring two degrees of freedom in the system. Therefore, the results of this particular study show power consumption due to damped vibration in only the horizontal direction. Figure 28 shows the steps in the simplification process.

65

The values for the equivalent mass (M_e, mass of the motor participating in the vibration), the spring stiffness (k), and damping were found experimentally by examining the transient response of the UTK motor set-up to an impulse excitation in the horizontal direction (shown in Figure 29). The same equipment (accelerometers, data acquisition systems) used in the project were used in this experiment to record the system's response. The damping coefficient was calculated using the log decrement method [Thomson 1981]. This entailed analyzing the decay of a transient signal after an impulse force was applied and approximating the rate of decrease as an exponential decay. With the best fit approximation for the decay envelope along with the natural frequency of the system (ω) determined from experimental data, Equation 5 can be used to find the damping coefficient (ζ) of the system. The damping coefficient for the system was found to be about 0.02. This value matches expectations and is in agreement with damping coefficient values for structural metals like aluminum and steel.
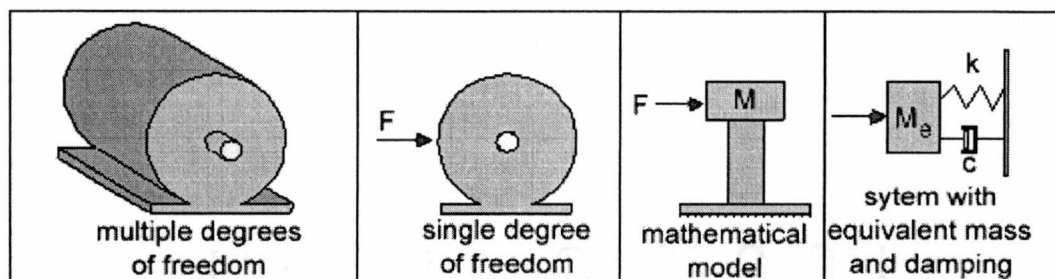
Figure 28: Simplification of motor vibration model

66
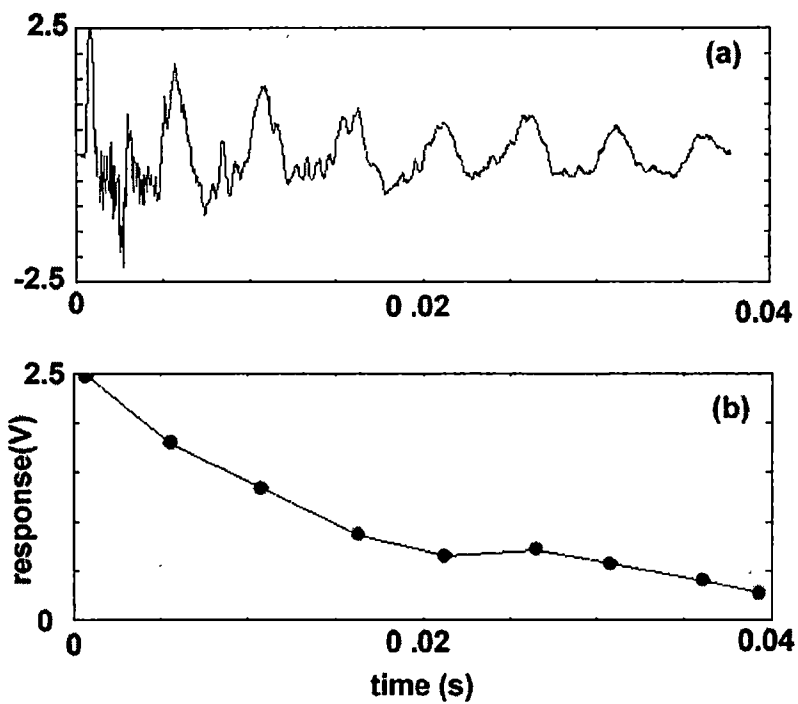
Figure 29: Vibration data used to determine damping and natural frequency of the motor system where (a) is the transient response of motor vibration and (b) is the envelope tracing the logarithmic decay

67

$$x(t) = A \cdot e^{-\zeta \cdot \omega \cdot t}$$

Equation 5

To find the stiffness of the motor, a second experiment was performed in which the mass of the motor was increased by a known amount and the natural frequency for this new system was calculated.   Equation **6** and Equation 7, which relate mass and stiffness to natural frequency, were solved simultaneously to find the stiffness (k) of the motor in the horizontal direction.

$$\omega_1^2 = \frac{k}{m_{eq}}$$

Equation 6

$$\omega_2^2 = \frac{k}{m_{eq} + m_{known}}$$

Equation 7

Values for displacement (x) were taken from experimental data archived. Equation 4 can now be used to calculate the power dissipated during vibration. The power loss was found to be about .0017 Watts out of the 49000 Watts powering the motor. This experiment can be used to calculate power loss in vertical and axial directions as well, and the order of magnitude of the results would not be much different. It is clear that increased vibration of the magnitudes seen in these tests can have no appreciable, much less measurable, effect on motor efficiency. In fact, by using the results of this analysis it can be shown that in order to produce a 1% change in efficiency the displacement in the horizontal plane would need to be 1.3 inches.

4.1.6 Comparison of Results with Previous Research for Motor Efficiency

As stated earlier, previous experimentation took place in situations where various disturbance to motor performance could not be measured or controlled well. Generally, the test results were derived based on assumptions of constant load on the motor and constant input voltages. Testing at UTK showed that these are likely to be invalid assumptions. On a typical day, line current could vary between 63.0 amps and 69.2 amps (a 9.8% difference) and line voltages could fluctuate between 462.1 volts and 455.7 volts (a 1.4 % difference). If output power were not measured, it is clear that, unless line voltages and currents were tightly controlled, reliable efficiency measurements could not be made.

Also, previous tests made no mention of insuring that the motor was held at steady state operating conditions during power consumption measurements. Experience has shown that factors such as temperature which determine steady state operation do have a large impact on motor efficiency, and, if not regulated closely, can interfere with efficiency measurements.

Some previous results do to some degree agree with the results of this testing in quantity but claim that power loss due to misalignment can be significant. In the case stated earlier where efficiency testing for a small 3 hp motor operating under misaligned conditions was performed, it was shown that a coupling in a misaligned state can consume (not transmit) between .01 and .03 hp more power than the same

69

coupling operating in an aligned condition. These are relatively small values to measure and certainly much smaller that the resolution of the measurement equipment at the UTK or ORNL facilities. Furthermore, a loss of .03 hp for a large 60 hp motor is insignificant. Generally, there are other factors in a plant such as operating temperature and line currents and voltages that can play a much greater role in motor efficiency than poor motor alignment. Another case in which previous research claimed significant monetary loss due to decreased efficiency of misaligned motors was the theoretical model of angularly misaligned machinery. In this case, improved alignment showed only about a 0.3% change. This model was based on several possibly invalid assumptions, but if this is ignored, the results still fall in closer accord with the results in this report (insignificant and immeasurable changes in efficiency) than with claims of notable power savings.

4.2 Results of Static and Steady State Bearing Load Testing

The results from the static and steady state testing will be discussed together. The analysis of the data for these two sets of tests was performed in very similar manners, and the comparison of these two sets of results lends insight into the influence that angular motion of the shafts and torque on the shafts have in the operation of the of the flexible couplings.

4.2.1 Discussion of Coupling Spring Rate

The analysis and the application of the results gathered in this study assume that the couplings used in this research can be modeled as a combination of several linear and

70

torsional springs. This means that any misalignment between two coupled shafts can be considered to be either a linear or angular displacement, and the coupling is a spring which generates a force and moment proportional to these displacements. The ratio of the force and/or moment induced by the coupling to the displacement is the spring rate ($k_{coupling}$) for the coupling (Equation 8).

$$k_{coupling} = \frac{force(\,or\ moment)}{misalignment}$$

Equation 8: Coupling Stiffness Relation

Both offset and the angular misalignments have been shown to result in the generation of a combination of a transverse force and a moment at the coupled end of the shaft. Therefore, there are four spring rates required to describe the functioning of a given coupling:

$k_{o,f}$ - spring rate relating <u>force</u> to <u>offset</u> misalignment   (lbf./mil)

$k_{o,m}$ - spring rate relating <u>moment</u> to <u>offset</u> misalignment   (lbf.-in./mil)

$k_{a,f}$ - spring rate relating <u>force</u> to <u>angular</u> misalignment   (lbf./ (mil/10 in.))

$k_{a,m}$ - spring rate relating <u>moment</u> to <u>angular</u> misalignment (lbf.-in./(mil/10 in.))

If these four constants are known for a specific coupling, the bearing loads induced by misalignment can be calculated for any size motor and for any given misalignment

71

condition. The methods for applying these spring rates are relatively simple and will be discussed later.

The spring rates for a given coupling were determined from the static and steady state test results. They were first calculated by determining the amount by which forces at the inboard and outboard bearings varied with purely angular and purely offset misalignments. This relationship is the slope of the best fit linear equation between the data points. Figure 30 is an example of how the force rate was determined.

With the force rates for the inboard and the outboard bearings known, a simple force (rate) balance equation for the system could be used to determine the force and moment rates (spring constants) of the flexible coupling. A diagram of this force balance is shown for the case of pure offset (Figure 31). The same approach is used for determining the two spring rates for angular misalignments. For this case, the equations would be changed so that $k_{o,m}$ and $k_{o,f}$ would be replaced by $k_{a,m}$ and $k_{a,f}$.

One important point to be made here is that the use of the term "spring stiffness" and the analogy between coupling stiffness and spring stiffness is not entirely in accordance with the classical definition of a spring. By definition, a spring exhibits a force when displaced, and the direction of that force is opposite that of the displacement and its magnitude is proportional to the displacement. In the model
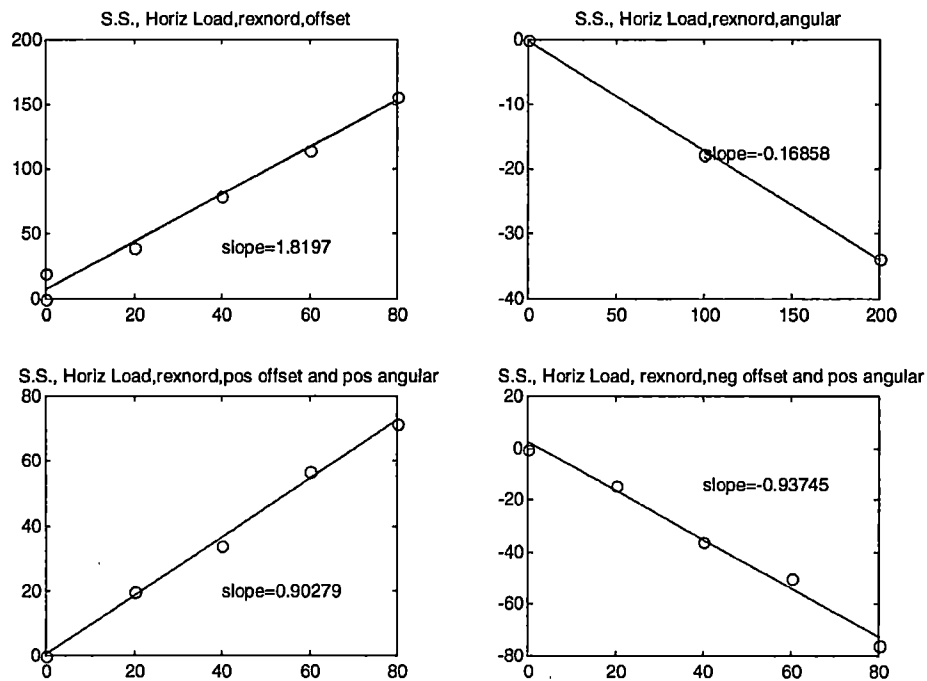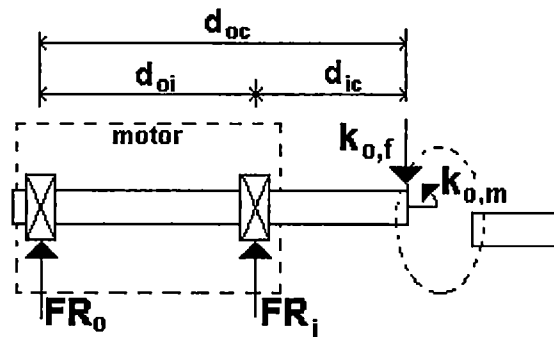
Figure 30 : Example of data relating misalignment to inboard bearing load for

Rexnord coupling

$$\sum M_c = 0, \quad \left(FR_o \cdot d_{oc}\right) + \left(FR_i \cdot d_{ic}\right) = k_{o,m}$$

$$\sum F = 0, \quad FR_o + FR_i = k_{o,f}$$

Figure 31: Force balance for offset misalignment

73

discussed so far, the results of the force balancing equation sometimes give negative

spring constants. This is counter-intuitive when considering normal springs. A

negative spring constant would suggest, for instance, that if one were to compress a

spring, the spring would react by creating a force that would cause it to compress

even further. The analogy to spring constants used in this discussion simply provides

a way to linearly relate measured forces to actual misalignments. It serves as a

convenient method of generalizing the specific test results from the specific motor

used in this test setup to any size motor. For instance, a negative spring constant $k_{o,m}$

would mean that a positive offset misalignment would cause the coupling to induce a

negatively defined moment at the end of the shaft.

4.2.2 Condensed Tables of Coupling Spring Rate Data

The two tables below show the calculated coupling spring rates for the four

couplings. Table 11 shows the results from static test situations in which the motor

was not moving, and Table 12 shows the measured coupling stiffness constants for

cases when the motor was running at full speed and under full load.

One important observation to be made in looking at this data is that the measured

spring rates for a given coupling are different when the coupling is motionless and

when it is spinning at full speed. There are several possible reasons for the

discrepancies in coupling response at different rotational speeds and these are related

to the particular construction of a given coupling.

74

Table 11: Coupling stiffness constants for static test case

Coupling Type	k (static)			
	Offset, Force lbf/mils	Offset, Moment in-lbf/ mil	Angular, Force lbf/(mil/10 in)	Angular, Moment in-lbf/(mil/10 in)
Rexnord	0.72	2.16	-0.05	2.45
Link	4.23	16.71	-0.15	3.09
Grid	15.17	88.25	1.44	17.26
Gear	0.73	13.08	0	0

Table 12: Coupling stiffness constants for steady state test cases

Coupling Type	k (steady state)			
	Offset, Force lbf/mils	Offset, Moment in-lbf/ mil	Angular, Force lbf/(mil/10 in)	Angular, Moment in-lbf/(mil/10 in)
Rexnord	1.65	6.17	-0.1	0.83
Link	4.73	-11.32	-0.24	5.13
Grid	19.54	4.53	0.74	-4.6
Gear	2.8	-1.86	-0.16	4.36

The most prominent influence that motion can have on a coupling is on the friction between surfaces in contact within the coupling. This friction can exhibit itself as a binding force which would result in a higher spring constant at no speed, but as speed increases, the static friction is diminished as well as the binding effect which it produces. This trend can be seen in the grid coupling results, in which internal binding between coupling components made the coupling far less forgiving to misalignment and thus resulted in higher bearing loads.

Internal friction can play another role and produce an opposite trend in the results. Kinetic friction resists motion between moving surfaces, and therefore would be nonexistent at zero speed and would only play a role as speed increases. This effect was evident in the gear coupling in which misalignment induced forces were virtually undetectable in static cases, but did affect bearing loads when the coupling was spinning. This trend was reversed in the grid coupling, where the effect of binding masked this. The other two couplings do not have slip planes and friction between moving surfaces does not play a role.

Operating temperature increase can also change coupling behavior. The steady state operating temperature of the couplings is generally between about 20°F to 30°F higher than those at ambient room temperature. Temperature changes can affect lubrication in the cases of the gear and grid coupling, and can also change polymer

resilience in the elastomeric coupling. All of these temperature dependent changes do affect the measured coupling stiffness.

From this evidence, it is clear that results testing the stiffness of a coupling under static testing can give no reliable prediction of its behavior under real operating conditions. In order to know what forces a coupling induces while within its intended operating conditions, one must test this coupling under those very same conditions. For this report, only the coupling stiffness values derived from steady state operating conditions will be considered in computations regarding bearing life.

4.2.3 Using Bearing Load to Determine Roller Element Bearing Life

The information given thus far has related shaft misalignment to bearing load. A further relationship can be developed in order to determine bearing life for roller element bearings as a function of the additional load caused by shaft misalignment through a coupling. Bearing manufacturers provide a load capacity ratings (C) which can be used to estimate bearing life (H) for a specific bearing operating under a specific load (L) and rotational speed (RPM). Equation 9 [Harris 1984] relating speed, capacity, load, and life is shown below:

$$H = \left(\frac{C}{L}\right)^3 \cdot \left(\frac{16667}{RPM}\right)$$

Equation 9: Bearing life equation

77

A more complicated and encompassing bearing life expectancy equation is shown in Equation 10, in which bearing loads incurred by vibration are calculated and added to constant loads. The constant loading is divided into two parts: load that is ever-present and due primarily to the design of the machine, and load generated exclusively by misalignment. This equation can be found in the literature, and the derivation of this equation is shown in the appendix.

$$H = \left(\frac{C}{L_{ma} + L_o + 6.77 \cdot 10^{-5} \cdot M \cdot V \cdot F} \right)^3 \cdot \left(\frac{16667}{RPM} \right)$$

C = Bearing capacity (lbf)
L_{ma} = Load due to misalignment (lbf)
L_o = Constant load on bearing present regardless of alignment or vibration
H = Bearing life expectancy (hr)
M = Mass opposing vibration (lbm)
V = Velocity of vibration (in/sec)
F = Frequency of vibration (RPM)

Equation 10: Bearing life based on constant and vibrational loading

A ratio between the estimated life of a bearing in a perfectly aligned case and a misaligned case can give a description of the reduction of useful life of a bearing operating in misaligned conditions. The "remaining life factor" is a positive value less than or equal to unity. The product of this factor and the maximum estimated life of the bearing (under perfectly aligned conditions) will give a new estimate on the life of the bearing under a misaligned condition. For instance, if the remaining life factor was calculated to be 0.6, then one could expect that the bearing would last only 60% as long as compared to an aligned conditions. In such a case, 40% of the operating life of the bearing was lost due to misalignment. This factor (given in Equation 11)

shows plainly the impact of improper alignment on the potential operating life of machinery.

$$\text{Remaining Life Factor} = \left(\frac{L_o + 6.7753 \cdot 10^{-5} \cdot M \cdot V \cdot F}{L_{ma} + L_o + 6.7753 \cdot 10^{-5} \cdot M \cdot V \cdot F} \right)^3$$

Equation 11

4.2.4 Test Data Results Applied to Roller Element Bearing Life Calculations

It is now possible to relate bearing life expectancy to shaft misalignment. In this section, the results from the steady state tests on inboard bearing loads will be used to determine what percentage of useful bearing life (possible if there were no misalignment) is lost when the roller element bearings are operated in misaligned conditions.

Figure 32a shows a three dimensional plot of the load measurements for the link coupling. The angular and offset misalignments are varied over the horizontal axes, and the vertical axis plots the bearing load at a given misalignment. Only about 100 of the data points shown in this graph were measured directly, the remainder were generated by spline interpolation between the known points. Equation 11 was then used with the data from Figure 32a to generate Figure 32b showing what percentage of inboard bearing life can be expected for a given misalignment condition. For this plot, the constants describing motor operating conditions are shown in Table 13.

79
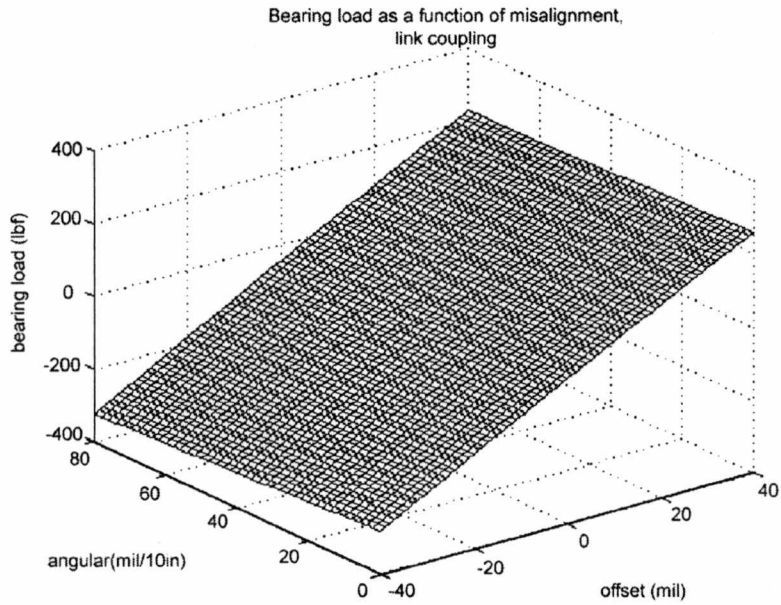
(a)
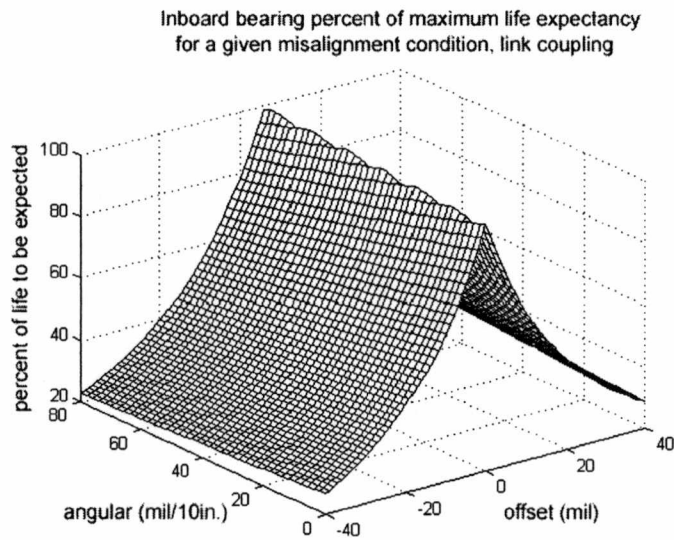
(b)

Figure 32: Maps for link coupling showing (a) bearing load as a function of angular and offset misalignment, (b) percentage of possible bearing life to be expected for a given angular and offset misalignment

80

Table 13: Constants used in bearing life estimation

RPM	3600 rpm
Mass	1000 lbs.
F	7200 CPM
C	18400 lbs.
V	0.012 in/sec.
Lo	500 lbs.

Figure 33 is a contour plot that shows the information in Figure 32 more clearly. The contours trace lines of constant percent life expectancy. One striking feature of this plot is that there are no closed regions specifying a finite range of operation enclosing a specific life expectancy range. This map, for instance, predicts the same life expectancy (100 %) for a bearing operating in a perfectly aligned case as one operating with an offset of +5 (mils) and an angularity of +80 (mils/10in). This means that for a specific bearing and coupling there exist certain combinations of angular and offset misalignment which cause bearing loads induced by angular misalignment to cancel those caused by offset misalignment. It is important to note that this cancellation only occurs at the one bearing where measurements are made. The other bearing in the motor does still feel a load. It would be impractical to use the data in Figure 33 to establish standards for machine alignment. A simple way to use the above data is to take a reflection of the data around the zero offset misalignment axis. This serves to create clear suggested operating regions for machinery for a given desired level of bearing reliability. Figure 34 through Figure 37 show these operating regions for the four different types of couplings used in this reasearch for the operating conditions specified in Table 13.

81
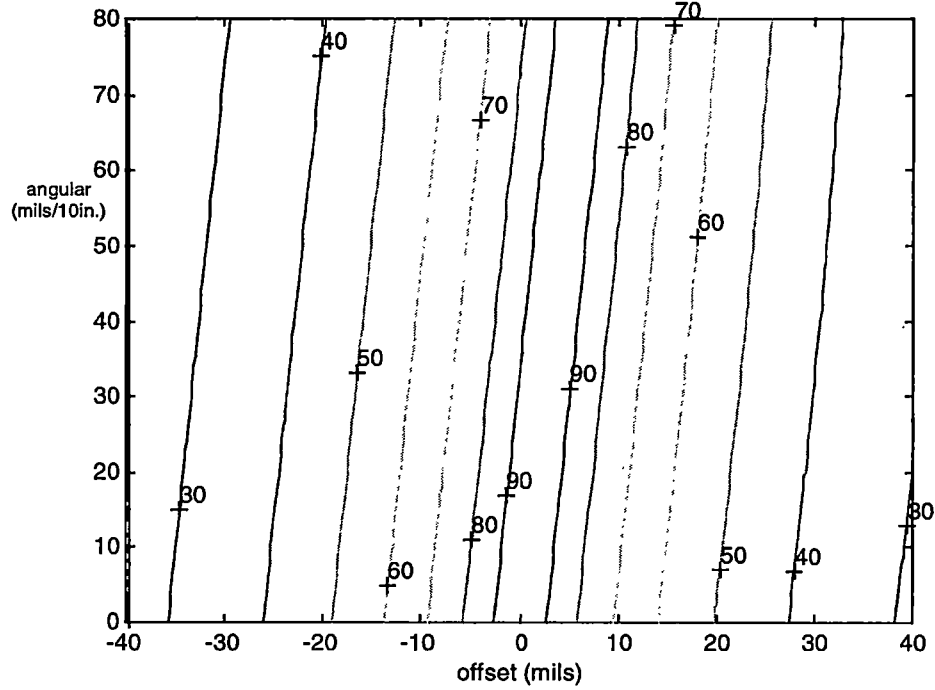
Figure 33: Contour plot of bearing life expectancy mapped against misalignment

conditions

Figure 34: Contour plot showing alignment operating regions for a given bearing life

expectancy for the link coupling

Figure 35: Contour plot showing alignment operating regions for a given bearing life

expectancy for the Rexnord elastomeric coupling

83

Figure 36: Contour plot showing alignment operating regions for a given bearing life
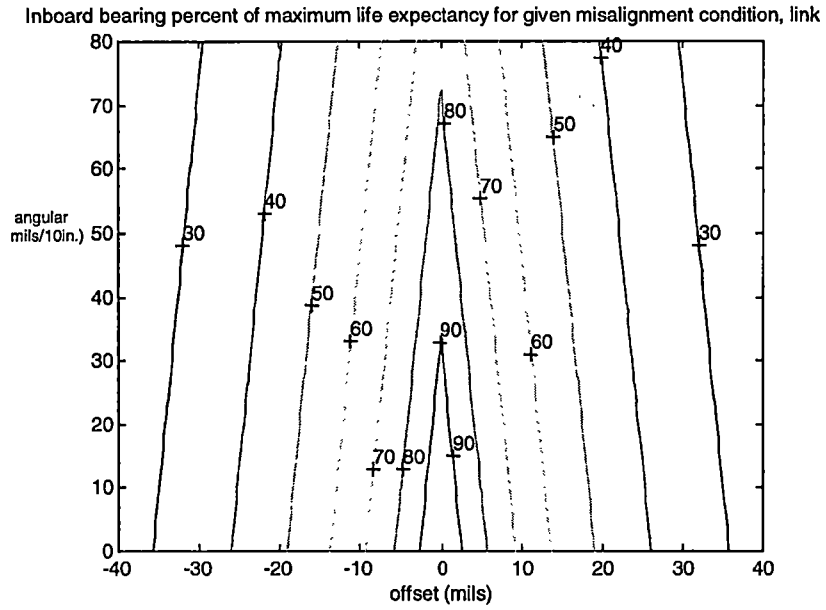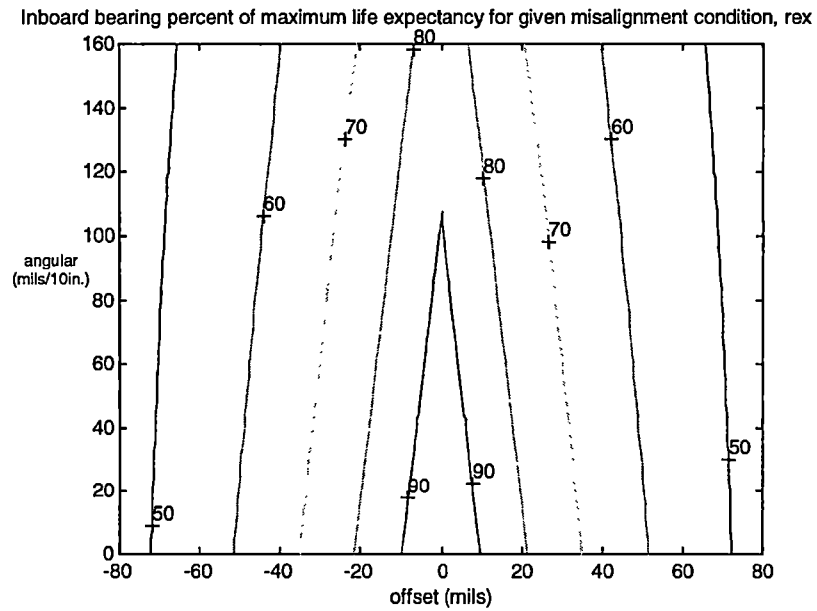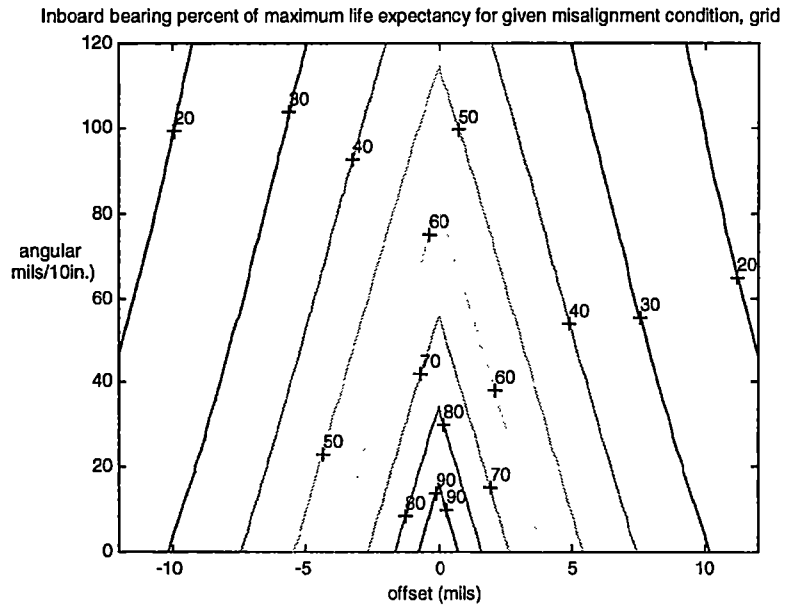expectancy for the grid coupling
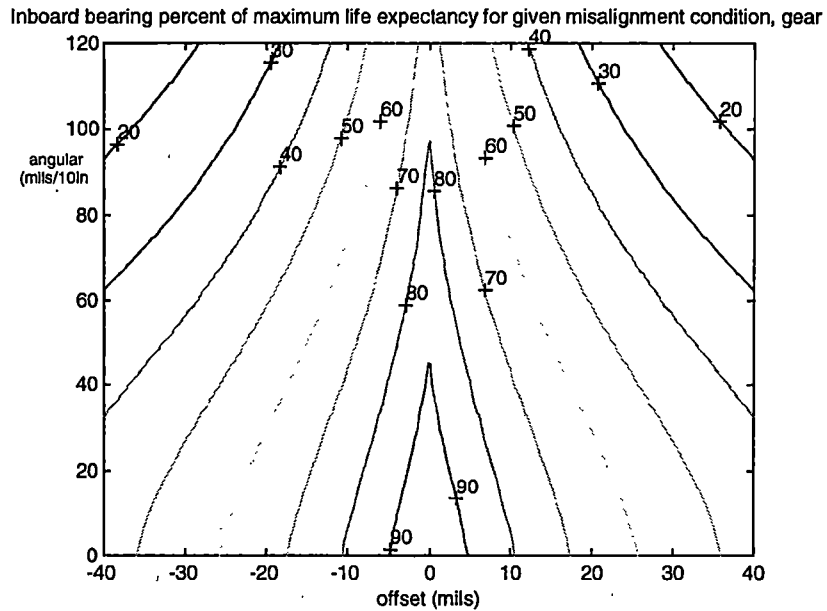
Figure 37: Contour plot showing alignment operating regions for a given bearing life
expectancy for the gear coupling

4.2.5 Consideration of Misalignment in the Vertical Plane

All of the results in this study were determined exclusively by examining the effects of misalignment in the horizontal plane. By exploiting the radial symmetry in rotating machinery, these results can easily be extended to encompass misalignments in the vertical direction as well as combined horizontal/vertical components. This is performed by simple vector addition as shown in Equation 12.

$$\text{offset} = \sqrt{\left(\text{offset}_{\text{horiz.}}\right)^2 + \left(\text{offset}_{\text{vert.}}\right)^2} \qquad \text{(a)}$$

$$\text{angular} = \sqrt{\left(\text{angular}_{\text{horiz.}}{}^2\right) + \left(\text{angular}_{\text{vert.}}\right)^2} \qquad \text{(b)}$$

Equation 12

The values for the combined offset and angular misalignments from these calculations can be used in all of the bearing load and life calculations discussed so far. In order for Equation 12 b to be used properly, the angular misalignment must be given in units of length/length (for instance mils/10 in.) and not in radial units such as degrees or radians.

5.0 Conclusions

5.1 Conclusions Regarding Efficiency

Careful measurements of motor position, motor power input, and motor power output have shown there to be no significant measurable correlation between shaft alignment and motor efficiency within the tested ranges of misalignment.

5.2 Conclusions Regarding Bearing Load

Steady state and stationary measurements were performed on a 60 HP motor that was coupled to a dynamometer with by four different couplings and showed that the couplings exhibit different reaction forces for the same alignment condition depending on whether the coupling was in motion or not. Therefore, measurements of coupling stiffness at zero speed cannot be extrapolated to determine coupling behavior under operating conditions.

The results from this research show that, for the couplings used in this testing, moderate shaft misalignments induce bearing loads that are large enough to have a significant impact on the life of the bearings. These increased loads are apparent in increased vibration and increased bearing and coupling temperatures.

The addition of load measuring bearings to commercial motors may be useful as an on-line measuring system to detect rotational imbalance and misalignment. This could assist in moving from periodic maintenance strategies to condition based maintenance strategies and could also assist in the diagnosis of problematic equipment.

5.2.1 Discussion of Angularity

All of the couplings used in this research show that angular misalignment has a much smaller impact on bearing life than offset misalignment does. Angular misalignment may in fact play a more significant role in reducing bearing life than this study suggests.

It is a commonly held belief that a flexible coupling operating in an angular misaligned state will induce an oscillatory axial load on the coupled shafts. This belief is substantiated by practical experience in that a commonly used method of diagnosing angular misalignment in rotating machinery is done by detecting excessive axial vibration. The bearing load sensors used in this research project could not detect this axial loading (only transaxial bearing loads were measured in this research) and, therefore, could not be used to measure the oscillatory thrust loads on the bearings.

It is suspected that the transaxial load measurements alone do not fully describe the degrading impact that angular misalignment has on bearings. It is likely that angular

misalignment can decrease bearing life further by inducing an additional load in the axial direction. The results in this project which estimate of the adverse impact that angular misalignment has on bearing life should be considered a minimum estimate.

5.2.2 General Guidelines in Alignment

The results from this study can be further condensed and generalized into a convenient set of "thumb rules". Table 14 shows how many mils of offset misalignment can be tolerated in order to remain within certain regions (90%, 80%, and 50%) of maximum possible life expectancy. These tolerable offset magnitudes are then normalized by the coupling manufacturer's specified maximum offset. It can then be broadly stated for the couplings used in this study that:

-if the motor is offset misaligned by 10% of the coupling manufacturer's allowable offset, then one can expect a 10% reduction in inboard bearing life

-if the motor is offset misaligned by 20% of the coupling manufacturer's allowable offset, then one can expect a 20% reduction in inboard bearing life

-if the motor is offset misaligned by 70% of the coupling manufacturer's allowable offset, then one can expect a 50% reduction in inboard bearing life

Table 14: Rules of thumb for offset misalignment and inboard bearing life

	Mills of offset for life expectancy:						
	90% of Life	80% of Life	50% of Life	Max offset	90% life/max off	80%life/max off	50%life/max off
Link	3	5	20	26	12%	19%	77%
Rex	8	21	70	70	11%	30%	100%
Grid	1	2	5	12	8%	17%	42%
Gear	5	10	35	50	10%	20%	70%
				avg =	10%	21%	72%

References

Computational Systems Inc., 835 Innovation Drive, Knoxville, TN 37932-2470,(423)-675-2110

Daintith, E., Glatt, P., "Reduce Costs with Laser Shaft Alignment." *Hydrocarbon Processing*, August 1996.

Emmery, J., Stidham, E., " Maintenance Task Assesment and Selection," *Reliability*, Vol. 2, No. 6, pp. 11-18, April 1996

Gaberson, H.A., and R Cappillino, "Rotating Machinery Energy Loss Due to Shaft Misalignment", Proceedings of the Society for Machinery Failure Preventive Technology, Virginia Beach, VA. Pp. 519-428, March 30 – April 2, 1998

Hines, J. W., S. Jesse, J. Kuropatwinski, T. Carley, J. Kueck, D. Nower, and F. Hale, "Motor Shaft Alignment Versus Efficiency Analysis", published in P/PM Technology, October, 1997, and presented at the P/PM Technology Conference, Dec. 1-4, 1997, Dallas, TX.

Hines, J.W, S. Jesse, A. Edmondson, D. Nower, "Motor Shaft Misalignment Versus Bearing Load Analysis", Maintenance Technology, May 1999

Hines J.W., D. Nower, S. Jesse, "Motor Shaft Misalignment Bearing Load Analysis", Reliability Magazine, June 2000

Harris, T.A, Roller Bearing Analysis. John Wiley & Sons Inc., New York, NY, 1984, p 457

Incropera, Frank P., Dewitt, David P., Fundamentals of Heat and Mass Transfer. John Wiley & Sons, New York, NY, 1990.   p 386 - 408

Kueck, John D., Casasa Donald A., Otaduy, Pedro J., "A Comparison of Two Energy Efficient Motors". *P/PM Technology*, April 1996

Ludeca Inc. Maintenance Study, "Evaluating Energy Consumption on Misaligned Machines". 1994.

Ludeca Inc., 1527 N.W. 89th Court, Miami, FL 33172, (305) 591-8935

Nower, D., "Misalignment: Challenging the Rules." *Reliability Magazine*, May/June 1994, p 38-43

Pardue, F., Piety, K.R., "Elements of Reliability Based Maintenance: Future Vision for Industrial Management," *CSI 1996 User Cenference Procedings*, Computional Systems, Inc., Nashville, TN,1996

Piotrowski, J., Monson H., Sweet G., Stomierosky B., Sullivan R., "Predictive Maintenance Technology National Conference, Panel Discussion." *P/PM Technology* , Feb. 1993.

Piotrowski, John. Shaft Alignment Handbook. Marcel Dekker Inc, New York, NY, 1995

Thomson, William T., Theory of Vibrations With Applications. Prentice Hall, Englewood Cliffs, NJ, 1981. p 69, p 30 – 34

Watkins, J., "Just in Time Maintenance Drives Just in Time Manufacturing," *Plant Services*, Vol. 17, No. 10, pp. 83-84, October 1996.

Weiss, W., "Laser Alignment Saves Amps, dollars." *Plant Services*, April 1991.

Xu, M., Zatezalo, J.M., Marangoni R.D., " Reducing Power Loss Through Shaft Alignment." *P/PM Technology*, October 1993.

Appendices

Estimates of Uncertainty in Efficiency Measurements at UTK

$$\text{efficiency} = \frac{P_{out}}{P_{in}} = \frac{v \cdot T}{P_{in}}$$

equation for efficiency
Pout = output power
Pin = input power
v = rotational velocity
T = Torque

$P_{in} := 50 \cdot kW$ $v := 3550 \cdot rpm$ $T := 550 \cdot ft \cdot lbf$ (approximate values for power, torque, and speed

$u_{pin} := .25 \cdot kW$ $u_v := 0.5 \cdot rpm$ $u_T := 0.5 \cdot ft \cdot lbf$ (uncertainty in these values

$$u_e = \sqrt{\left[\left(\frac{d}{dP_{in}}eff\right)\cdot u_{pin}\right]^2 + \left[\left(\frac{d}{dv}eff\right)\cdot u_v\right]^2 + \left[\left(\frac{d}{dT}eff\right)\cdot u_T\right]^2}$$ (uncertainty in efficiency)

$$\frac{d}{dP_{in}}eff = \frac{d}{dP_{in}}\left(\frac{v \cdot T}{P_{in}}\right) = \frac{-v \cdot T}{P_{in}^2}$$ $$\frac{d}{dv}eff = \frac{d}{dv}\left(\frac{v \cdot T}{P_{in}}\right) = \frac{T}{P_{in}}$$ $$\frac{d}{dT}eff = \frac{d}{dT}\left(\frac{v \cdot T}{P_{in}}\right) = \frac{v}{P_{in}}$$

$$u_e := \sqrt{\left(\frac{-v \cdot T}{P_{in}^2} \cdot u_{pin}\right)^2 + \left[\left(\frac{T}{P_{in}}\right)\cdot u_v\right]^2 + \left[\left(\frac{v}{P_{in}}\right)\cdot u_T\right]^2}$$

$u_e = 4.486 \cdot 10^{-3}$ uncertainty in efficiency measurements

93

Calculations of Power Loss Due to Heat Loss

Assumed dimensions of shaft:
length = 40 cm
diameter = 12 cm

Angular Velocity = 3600 rpm
Temperature Change due to misalignment = 3 degrees Celcius

Properties of air at 300 K

$$v = 15.89 \cdot 10^{-6} \ m^2/s \qquad k = 26.3 \cdot 10^{-3} \ W/mK \qquad P_r = .707$$

Velocity of air seen by shaft

$$V_{inf} = (3600) \cdot \left(\frac{1}{60}\right) \cdot (\pi \cdot .12) \qquad\qquad V_{inf} = 22.6 \quad m/s$$

Length of plate (circumference of shaft)

$$L = .12 \cdot \pi \qquad\qquad L = .38 \quad m$$

Find Reynold's number

$$Re_L = \frac{V_{inf} L}{v} = \frac{(22.6) \cdot (.38)}{15.89 \cdot 10^{-6}} \qquad Re_L = 540465 \quad \text{(turbulent flow)}$$

Find Nusselt number

$$Nu_x = .0296 \left(Re_L^{.8}\right) \cdot Pr^{(.33)} = .0296 \left(540465^8\right) \cdot .707^{(.33)}$$

$$Nu_x = .0296 \left(Re_L^{.8}\right) \cdot Pr^{(.33)} = 1018.15$$

Find the coefficient of convective heat transfer

$$h_L = \frac{Nu_x \cdot k}{L} = \frac{1018.15 \left(26.3 \cdot 10^{-3}\right)}{.38} \qquad h_L = 70.5 \quad W/m^2{}^*K$$

Find change in heat transfer due to difference in surface temperatures

$$\Delta q = h_L \cdot (L) \cdot (\text{Width}) \cdot \left(T_{s1} - T_{s2}\right) = 70.5 (.38) \cdot (.4) \cdot (3)$$

$$\Delta q = 32.13 \quad \text{Watts}$$

Percentage of total power lost as increase in temperature of shaft

$$\left(\frac{32.13}{49000}\right) \cdot 100 = .065 \quad \% \ \text{change}$$

94

Calculations of Power Loss Due to Damping of Vibration

Solving for coefficients of log decrement equation

$$x(t) = A \cdot e^{-\zeta \omega \cdot t} = A \cdot e^{-K \cdot t}$$

acceleration
$$= \frac{d^2}{dt^2} x(t) = \frac{d^2}{dt^2} A \cdot e^{-K \cdot t} = A \cdot K^2 \cdot e^{-K \cdot t}$$

Given data from transient analysis:

acceleration $= .5e^{-50 \cdot t}$

$\omega_n = 2618$ rad/sec $\qquad\qquad K^2 \cdot A = .5$

$K = \zeta \cdot \omega = 50$ $\qquad\qquad A = 2 \cdot 10^{-4}$

$\zeta \cdot 2618 = 50$

$\zeta = .019$

Equation for power consumption per cycle:

$$W_d = \pi \cdot \zeta \cdot \beta \cdot k \cdot x^2 \qquad \text{where} \qquad \beta = \frac{\omega}{\omega_n}$$

This rquires that a value for k be found

> k can be found by measuring the natural frequency of the system,
> and measuring the natural frequency of the system with an increased mass
> where the added mass is known.

$\omega_1 = 2618$ rad/sec $\qquad m_1 = m_e$ (equivalent mass, slugs)

$\omega_2 = 1257$ rad/sec $\qquad m_2 = m_e + 1.55$

$$\omega_n{}^2 = \frac{k}{m}$$

$$\omega_1{}^2 = 2168^2 = \frac{k}{m_e} \qquad\qquad \omega_2{}^2 = 1257^2 = \frac{k}{m_e + 1.55}$$

This yields:

$k = 3.816 \cdot 10^6$ lbf/ft $\qquad\qquad m_e = .685$ slugs

Using velocity data from experimentation to find displacements

$V_{align} = .011$ in/sec $\qquad\qquad V_{misal} = .012$ in/sec

$$x = \frac{V}{\zeta \omega}$$

$x_{align} = 2.2 \cdot 10^{-4}$ in $\qquad\qquad x_{misal} = 2.4 \cdot 10^{-4}$ in

Solve for energy lost per unit cycle

$$W_d = \pi \cdot \zeta \cdot \beta \cdot k \cdot \left(x_{misal}{}^2 - x_{align}{}^2 \right)$$

95

Derivation of Bearing Life Equation Including Misalignment Load and Vibrational Load

The standard equation for L10 life is given in equation 9 as

$$H = \left(\frac{C}{L_{tot}}\right)^3 \cdot \left(\frac{16667}{RPM}\right)$$

Where C is the bearing rating, L.tot is the total load on the bearing, and RPM is the rotational speed of the bearing in rpm, H is the anticipated life of the bearing in hours.

Equation 10 divides L.tot into three different loads: Load due to misalignment (L.ma), Load due to the oscillatory motion of a mass (L.vib), and load the is ever-present and intrinsic to the design of the rotating equipment (L.o).

$$L_{tot} = L_{ma} + L_o + L_{vib}$$

L.vib is found by multiplying the oscillating mass by the velocity of the oscillation to find its momentum. This is multiplied by the frequency of oscillation to find the force.

This factor is scaled by units:

$$lb \cdot \frac{in}{sec} \cdot \frac{1}{min} = 4.32 \cdot 10^{-5} \circ lbf$$

Since the force is sinusoidal, we must consider the average load

$$\frac{1}{\pi} \cdot \int_0^\pi \sin(t)\, dt = 2 \cdot \frac{1}{\pi}$$

Average value for a sinusoid over one cycle

This is factored in with the units to give

$$lb \cdot \frac{in}{sec} \cdot \frac{1}{min} \cdot \frac{\pi}{2} = 6.78 \cdot 10^{-5} \circ lbf$$

Combining all this together gives:

$$H = \left(\frac{C}{L_{ma} + L_o + 6.78 \cdot 10^{-5} \cdot M \cdot V \cdot F}\right)^3 \cdot \left(\frac{16667}{RPM}\right)$$

Vita

Stephen Jesse was born in Boulder, Colorado on December 5, 1973. He graduated from Hendersonville High School in Hendersonville, Tennessee in 1992 and entered the engineering program that same year at the University of Tennessee, Knoxville. He completed the requirements for a Bachelor of Science degree in Mechanical Engineering in 1996.

Following the completion of this Masters of Science degree, Stephen plans to fulfill the requirements for a second Masters of Science degree in Materials Science, also from the University of Tennessee.